



Entergy Operations, Inc.
17265 River Road
Killona, LA 70057-3093
Tel 504 739 6660
Fax 504 739 6698
mchisum@entergy.com

Michael Chisum
Site Vice President
Waterford 3

W3F1-2014-0023

March 27, 2014

U.S. Nuclear Regulatory Commission
Attn: Document Control Desk
Washington, DC 20555-0001

SUBJECT: Entergy Seismic Hazard and Screening Report (CEUS Sites), Response To NRC Request for Information Pursuant to 10 CFR 50.54(f) Regarding Recommendation 2.1 of the Near-Term Task Force Review of Insights from the Fukushima Dai-ichi Accident.
Waterford Steam Electric Station, Unit 3 (Waterford 3)
Docket No. 50-382
License No. NPF-38

- REFERENCES:**
1. NRC Letter, "Request for Information Pursuant to Title 10 of the Code of Federal Regulations 50.54(f) Regarding Recommendations 2.1, 2.3, and 9.3, of the Near-Term Task Force Review of Insights from the Fukushima Dai-ichi Accident," dated March 12, 2012 (ADAMS Accession No. ML12053A340)
 2. NEI Letter, "Proposed Path Forward for NTTF Recommendation 2.1: Seismic Reevaluations," dated April 9, 2013 (ADAMS Accession No. ML13101A379)
 3. NRC Letter, "Electric Power Research Institute Final Draft Report XXXXXX, 'Seismic Evaluation Guidance: Augmented Approach for the Resolution of Fukushima Near-Term Task Force Recommendation 2.1: Seismic,' as an Acceptable Alternative to the March 12, 2012, Information Request for Seismic Reevaluations," dated May 7, 2013 (ADAMS Accession No. ML13106A331)
 4. EPRI Report 1025287, "Seismic Evaluation Guidance, Screening, Prioritization and Implementation Details (SPID) for the Resolution of Fukushima Near-Term Task Force Recommendation 2.1: Seismic," (ADAMS Accession No. ML12333A170)
 5. NRC Letter, "Endorsement of EPRI Final Draft Report 1025287, "Seismic Evaluation Guidance," dated February 15, 2013 (ADAMS Accession No. ML12319A074)

Dear Sir or Madam:

On March 12, 2012, the Nuclear Regulatory Commission (NRC) issued Reference 1 to all power reactor licensees and holders of construction permits in active or deferred status. Enclosure 1 of Reference 1 requested each addressee located in the Central and Eastern United States (CEUS) to submit a Seismic Hazard Evaluation and Screening Report within 1.5 years from the date of Reference 1.

In Reference 2, the Nuclear Energy Institute (NEI) requested NRC agreement to delay submittal of the final CEUS Seismic Hazard Evaluation and Screening Reports so that an update to the Electric Power Research Institute (EPRI) ground motion attenuation model could be completed and used to develop that information. NEI proposed that descriptions of subsurface materials and properties and base case velocity profiles be submitted to the NRC by September 12, 2013, with the remaining seismic hazard and screening information submitted by March 31, 2014. The NRC agreed with that proposed path forward in Reference 3.

Reference 4 contains industry guidance and detailed information to be included in the Seismic Hazard Evaluation and Screening Report submittals. The NRC endorsed this industry guidance in Reference 5.

The attached Seismic Hazard Evaluation and Screening Report for Waterford 3 provides the information described in Section 4 of Reference 4 in accordance with the schedule identified in Reference 2.

This letter contains no new regulatory commitments.

If you have any questions or require additional information, please contact John P. Jarrell at (504) 739-6685.

I declare under penalty of perjury that the foregoing is true and correct. Executed on March 27, 2014.

Sincerely,



MC/LEM

Attachment: Waterford 3 Seismic Hazard and Screening Report

cc: Attn: Director, Office of Nuclear Reactor Regulation
U. S. NRC
RidsNrrMailCenter@nrc.gov

Mr. Mark L. Dapas, Regional Administrator
U. S. NRC, Region IV
RidsRgn4MailCenter@nrc.gov

NRC Project Manager for Waterford 3
Alan.Wang@nrc.gov
Michael.Orenak@nrc.gov

NRC Resident Inspectors for Waterford 3
Marlone.Davis@nrc.gov
Chris.Speer@nrc.gov

Attachment to

W3F1-2014-0023

Waterford 3 Seismic Hazard and Screening Report

**Seismic Hazard and Screening Report
Waterford 3**

Table of Contents

| | Page |
|---|-------------|
| 1.0 Introduction | 3 |
| 2.0 Seismic Hazard Reevaluation | 4 |
| 2.1 Regional and Local Geology | 4 |
| 2.2 Probabilistic Seismic Hazard Analysis | 5 |
| 2.2.1 Probabilistic Seismic Hazard Analysis Results | 5 |
| 2.2.2 Base Rock Seismic Hazard Curves | 6 |
| 2.3 Site Response Evaluation | 6 |
| 2.3.1 Description of Subsurface Material | 7 |
| 2.3.2 Development of Base Case Profiles and Nonlinear Material Properties | 8 |
| 2.3.2.1 Shear Modulus and Damping Curves | 11 |
| 2.3.2.2 Kappa | 11 |
| 2.3.3 Randomization of Base Case Profiles | 12 |
| 2.3.4 Input Spectra | 12 |
| 2.3.5 Methodology | 13 |
| 2.3.6 Amplification Functions | 13 |
| 2.3.7 Control Point Seismic Hazard Curves | 18 |
| 2.4 Control Point Response Spectrum | 19 |
| 3.0 Plant Design Basis and Beyond Design Basis Evaluation Ground Motion | 20 |
| 3.1 SSE Description of Spectral Shape | 21 |
| 3.2 Control Point Elevation | 22 |
| 3.3 IPEEE Description and Capacity Response Spectrum | 22 |
| 4.0 Screening Evaluation | 22 |
| 4.1 Risk Evaluation Screening (1 to 10 Hz) | 22 |
| 4.2 High Frequency Screening (> 10 Hz) | 23 |
| 4.3 Spent Fuel Pool Evaluation Screening (1 to 10 Hz) | 24 |
| 5.0 Interim Actions | 24 |
| 6.0 Conclusions | 25 |
| 7.0 References | 25 |
| Appendix A | 27 |

1.0 Introduction

Following the accident at the Fukushima Daiichi nuclear power plant resulting from the March 11, 2011, Great Tohoku Earthquake and subsequent tsunami, the Nuclear Regulatory Commission (NRC) established a Near-Term Task Force (NTTF) to conduct a systematic review of NRC processes and regulations and to determine if the agency should make additional improvements to its regulatory system. The NTTF developed a set of recommendations intended to clarify and strengthen the regulatory framework for protection against natural phenomena. Subsequently, the NRC issued a 50.54(f) letter (U.S. NRC, 2012) that requests information to assure that these recommendations are addressed by all U.S. nuclear power plants. The 50.54(f) letter requests (U.S. NRC, 2012) that licensees and holders of construction permits under 10 CFR Part 50 reevaluate the seismic hazards at their sites against present-day NRC requirements. Depending on the comparison between the reevaluated seismic hazard and the current design basis, the result is either no further risk evaluation or the performance of a seismic risk assessment. Risk assessment approaches acceptable to the staff include a Seismic Probabilistic Risk Assessment (SPRA), or a Seismic Margin Assessment (SMA). Based upon the risk assessment results, the NRC staff will determine whether additional regulatory actions are necessary.

This report provides the information requested in items (1) through (7) of the "Requested Information" section and Attachment 1 of the 50.54(f) letter (U.S. NRC, 2012) pertaining to NTTF Recommendation 2.1 for the Waterford Steam Electric Station 3 (WSES-3), located in St. Charles Parish, Louisiana. In providing this information, Entergy followed the guidance provided in the "Seismic Evaluation Guidance: Screening, Prioritization, and Implementation Details (SPID) for the Resolution of Fukushima Near-Term Task Force Recommendation 2.1: Seismic" (EPRI, 2013a). The Augmented Approach, "Seismic Evaluation Guidance: Augmented Approach for the Resolution of Fukushima Near-Term Task Force Recommendation 2.1: Seismic" (EPRI, 2013b), has been developed as the process for evaluating critical plant equipment as an interim action to demonstrate additional plant safety margin prior to performing the complete plant seismic risk evaluations.

The original geologic and seismic siting investigations for WSES-3 were performed in accordance with Appendix A to 10 CFR Part 100 and meet General Design Criterion 2 in Appendix A to 10 CFR Part 50. The Safe Shutdown Earthquake (SSE) Ground Motion was developed in accordance with Appendix A to 10 CFR Part 100 and used for the design of seismic Category I systems, structures and components.

In response to the 50.54(f) letter (U.S. NRC, 2012) and following the guidance provided in the SPID (EPRI, 2013a), a seismic hazard reevaluation was performed. For screening purposes, a Ground Motion Response Spectrum (GMRS) was developed. Based on the results of the screening evaluation, no further evaluations will be performed.

2.0 Seismic Hazard Reevaluation

The Waterford Steam Electric Station 3 is situated along the west (right descending) bank of the Mississippi River in Killona, Louisiana, about 25 miles west of New Orleans, Louisiana. It is located in the southern portion of the Gulf Coastal Plain geologic province. The southern portion of the Gulf Coastal Plain is the Mississippi River deltaic plain physiographic province. The site is underlain by sediments consisting of marine shales, sandstones and clays, and recent alluvium deposits which are described as soft clays and silty clays with occasional sand lenses or pockets. There is no cavernous or karst terrain in the site area. The sediments are not subject to stress build-up with formation of deformational zones or other structural weaknesses. With the exception of the recent alluvium, which was removed and replaced with compacted sand backfill, unstable conditions of the subsurface materials at the site due to mineralogy, lack of consolidation, or water content do not exist. The regional geologic structures in the deltaic plain consist of salt structures, their overlying attendant faults, and growth faults. The growth faults represent previously unstable areas which were at the leading slope of sediment accumulation. The subsurface data demonstrate that such regional structures cannot affect the WSES-3 site. (Entergy, 2013)

Earthquake activity in historic time within 200 miles of the plant site has been minor. The New Madrid series of earthquakes of epicentral Intensity XII on the Modified Mercalli Intensity Scale of 1931 and the Donaldsonville earthquake are probably the only seismic events that have been felt in the site and surrounding area during the past 250 years. The greatest intensity experienced at the site during the historic record was Intensity V on the Modified Mercalli Intensity Scale of 1931 or less. There is no physical evidence to indicate any earthquake effects at the site. In considering conditions in the selection of the SSE in Amendment to 10 CFR Part 100, Appendix A, the Licensee has concluded that they are not applicable to the WSES-3 site. Therefore, the SSE for the site is based on a hypothetical earthquake with epicentral Intensity VI on the Modified Mercalli Intensity Scale of 1931 occurring adjacent to the site. In order to comply with the minimum accepted acceleration as stipulated by Appendix A in 10 CFR Part 100, WSES-3 was designed for a maximum horizontal ground surface acceleration of 0.10g. This very conservative surface acceleration is double the maximum acceleration appropriate for the maximum earthquake which has occurred in the site's tectonic province during the past 250 years. The peak vertical acceleration for the postulated SSE is 2/3 peak horizontal acceleration. (Entergy, 2013)

2.1 Regional and Local Geology

The Waterford Steam Electric Station 3 is located in the southern portion of the Gulf Coastal Plain geologic province. The southern portion of the Gulf Coastal Plain is the Mississippi River deltaic plain physiographic province. The Mississippi River has dominated the development of geologic and physiographic features in the deltaic plain since the beginning of Neogene. The site is characterized by flat topography near sea level, with extensive areas covered by water, swamp, or marsh. In the site and surrounding area, the physiography is dominated by the present Mississippi River. (Entergy, 2013)

The Waterford Steam Electric Station 3 is located almost entirely upon the natural levee of the Mississippi River. The upper 500 feet of sediments within the site boundaries is characterized by nearly flat lying sediments which can be traced laterally by stratigraphic horizons. All seismic Category I structures are founded at elevation -47 ft Mean Sea Level (MSL) on a one foot thick compacted shell filter blanket on top of the Pleistocene clay. The excavation for the WSES-3 seismic Category I structural mat was cut 60 ft deep and exposed several feet of the Pleistocene Prairie formation. In the excavation, the Prairie formation at foundation level consists of horizontally bedded layers of silts and clays. Mapping of the excavation disclosed no anomalies or discontinuities which might indicate conditions which could adversely affect the integrity of the foundation materials. The contours of the surface of the Pleistocene show very little variation in a north-south direction where displacements would be expected if faulting were present. In addition to the relatively subdued contours of the top of the Pleistocene, contours of individual strata down to about -5000 ft show no indication of faulting. No zones of alteration or irregular weathering exist in the site area. Over 40,000 ft of mostly unconsolidated sediments lie above the crystalline basement rock beneath the site. No unrelieved residual stresses exist in the unconsolidated foundation materials. (Entergy, 2013)

2.2 Probabilistic Seismic Hazard Analysis

2.2.1 Probabilistic Seismic Hazard Analysis Results

In accordance with the 50.54(f) letter (U.S. NRC, 2012) and following the guidance in the SPID (EPRI, 2013a), a Probabilistic Seismic Hazard Analysis (PSHA) was completed using the recently developed Central and Eastern United States Seismic Source Characterization (CEUS-SSC) for Nuclear Facilities (CEUS-SSC, 2012) together with the updated Electric Power Research Institute (EPRI) Ground Motion Model (GMM) for the Central and Eastern United States (CEUS) (EPRI, 2013c). For the PSHA, a lower-bound moment magnitude of 5.0 was used, as specified in the 50.54(f) letter (U.S. NRC, 2012). (EPRI, 2014)

For the PSHA, the CEUS-SSC background seismic sources out to a distance of 400 miles (640 km) around WSES-3 were included. This distance exceeds the 200 mile (320 km) recommendation contained in Reg. Guide 1.208 (U.S. NRC, 2007) and was chosen for completeness. Background sources included in this site analysis are the following (EPRI, 2014):

1. Extended Continental Crust—Atlantic Margin (ECC_AM)
2. Extended Continental Crust—Gulf Coast (ECC_GC)
3. Gulf Highly Extended Crust (GHEX)
4. Mesozoic and younger extended prior – narrow (MESE-N)
5. Mesozoic and younger extended prior – wide (MESE-W)
6. Midcontinent-Craton alternative A (MIDC_A)
7. Midcontinent-Craton alternative B (MIDC_B)
8. Midcontinent-Craton alternative C (MIDC_C)

9. Midcontinent-Craton alternative D (MIDC_D)
10. Non-Mesozoic and younger extended prior – narrow (NMESE-N)
11. Non-Mesozoic and younger extended prior – wide (NMESE-W)
12. Oklahoma Aulacogen (OKA)
13. Paleozoic Extended Crust narrow (PEZ_N)
14. Paleozoic Extended Crust wide (PEZ_W)
15. Reelfoot Rift (RR)
16. Reelfoot Rift including the Rough Creek Graben (RR-RCG)
17. Study region (STUDY_R)

For sources of large magnitude earthquakes, designated Repeated Large Magnitude Earthquake (RLME) sources in NUREG-2115 (CEUS-SSC, 2012) modeled for the CEUS-SSC, the following sources lie within 1,000 km of the site and were included in the analysis (EPRI, 2014):

1. Charleston
2. Commerce
3. Eastern Rift Margin Fault northern segment (ERM-N)
4. Eastern Rift Margin Fault southern segment (ERM-S)
5. Marianna
6. Meers
7. New Madrid Fault System (NMFS)
8. Wabash Valley

The Gulf version of the updated CEUS EPRI GMM was used to model the seismic wave travel path from source to site for each of the above background sources. For RLME sources, a combination of Gulf and mid-continent GMMs was created to represent the relative fraction of the seismic wave travel path through these regions. To approximate the average path from each source, the relative fractions used were 60% for Gulf GMMs and 40% for mid-continent GMMs. (EPRI, 2014)

2.2.2 Base Rock Seismic Hazard Curves

Consistent with the SPID (EPRI, 2013a), base rock seismic hazard curves are not provided as the site amplification approach referred to as Method 3 has been used. Seismic hazard curves are shown below in Section 2.3.7 at the SSE control point elevation. (EPRI, 2014)

2.3 Site Response Evaluation

Following the guidance contained in Seismic Enclosure 1 of the 50.54(f) Request for Information (U.S. NRC, 2012) and in the SPID (EPRI, 2013a) for nuclear power plant sites that are not founded on hard rock (defined as 2.83 km/sec), a site response analysis was performed for WSES-3. (EPRI, 2014)

2.3.1 Description of Subsurface Material

The Waterford Steam Electric Station 3 is located along the west (right descending) bank of the Mississippi River about 25 miles (40 km) west of New Orleans, Louisiana. It is located in the southern portion of the Gulf Coastal Plain geomorphic province which is the Mississippi River deltaic physiographic province. The site is located almost entirely upon the natural levee for the Mississippi River. The upper 500 ft (152 m) of sediments are flat lying and consist of interbedded sands and clays with varying amounts of silt (Entergy, 2013). (EPRI, 2014)

The information used to create the site geologic profile at WSES-3 is shown in Table 2.3.1-1. This profile was developed using information documented in the Final Safety Analysis Report (FSAR) (Entergy, 2013). As indicated in Table 2.3.1-1, the SSE Control Point is defined at elevation -47 ft with Precambrian basement at a depth of greater than 40,000 ft (12,200m). The profile consists of about 4,900 ft (1,500 m) of soil overlying about 35,100 ft (10,700 m) of firm sedimentary rock. (EPRI, 2014)

Table 2.3.1-1 Summary of Geotechnical Profile for WSES-3. (Entergy, 2013)

| Depth Range (ft) | Elev. (ft) | Soil Description | Density (pcf) | Shear Wave Velocity (fps) | Compressional Wave Velocity (fps) ¹ | Poisson's Ratio |
|-------------------|--------------|---|---------------|---------------------------|--|-----------------|
| 0 – 55 | +15 to -40 | Clay and silty clay with silt and sand lenses (recent material) (included for information only) | 111 | N.A. | 3,000 ± 500 | 0.48 |
| SSE control point | -47 | - | - | - | - | - |
| 55 – 92 | -40 to -77 | Stiff tan and gray fissured clay | 119 | 850 | 5,700 ± 700 | 0.49 |
| 92 – 107 | -77 to -92 | Very dense tan silty sand | 125 | 925 | 5,700 ± 700 | 0.48 |
| 107 – 123 | -92 to -108 | Medium stiff gray clay with silt lenses | 119 | 925 | 5,700 ± 700 | 0.49 |
| 123 – 131 | -108 to -116 | Stiff dark gray clay – organic | 104 | 1,000 | 5,700 ± 700 | 0.49 |
| 131 – 142 | -116 to -127 | Soft to medium stiff tan and gray clay with sand lenses | 119 | 1,000 | 5,700 ± 700 | 0.49 |
| 142 – 332 | -127 to -317 | Very stiff clays with silts and sands | 119 | 1,100 – 1,150 | N.A. | 0.48 |
| 332 – 515 | -317 to -500 | Very dense sands and silty sands | 119 to 125 | 1,600 – 1,650 | N.A. | 0.45 |

¹ Uphole Seismic Survey.

NOTES: Foundation for nuclear island is at elevation -47 ft, MSL, at the top of the Pleistocene material. Top of grade is considered to be at elevation +15 ft, MSL.

The general geology of the site consists of the Pleistocene Prairie Formation interbedded with sands and clays with varying amounts of silt and extends to a depth of about 1,100 ft. The Pliocene – Pleistocene deposits consist of the Citronelle Formation of interbedded sands and clays that extend to about 1,900 ft. Beneath these strata are about 3,000 ft. of Pliocene clays with relatively thin sand layers. Between 7,500 and 10,500 ft. is a sequence of shale alternating with thin sandstone layers. This unit overlies a continuous sequence of shale ranging in age from middle to upper Jurassic. The lower Jurassic Louann salt beds are the deepest sediments known to occur above crystalline bedrock. Precambrian crystalline basement rock was estimated to be at a depth greater than 40,000 ft (Entergy, 2013).

2.3.2 Development of Base Case Profiles and Nonlinear Material Properties

Table 2.3.1-1 shows the recommended shear-wave velocities and unit weights versus depth and elevation for the best estimate single profile to a depth of 515 ft (157 m). Velocity measurements consist of compressional-wave uphole velocity surveys at the site to a depth below the SSE of about 173 ft (53 m) (Entergy, 2013). Recommended shear-wave velocities listed in Table 2.3.1-1 were taken as the mean base-case profile (P1) in the top 460 ft (140 m). Beneath this depth the profile was extended to a depth of 4,000 ft (1,219 m) using the average S-wave velocity over the upper 30 m (V_{S30}) of 270m/sec (886 ft/s) profile template from the SPID (EPRI, 2013a). The depth of 4,000 ft (1,219 m) was considered adequate to reflect amplification over the lowest frequency of interest, about 0.5 Hz (EPRI, 2013a). (EPRI, 2014)

Lower (P2)- and upper (P3)- range profiles were developed with scale factors of 1.25 reflecting uncertainty in measured velocities to a depth of 173 ft (53 m). Below this depth shear-wave velocities reflect assumed values and increased epistemic uncertainty with an increased scale factor of 1.57. To avoid development of a low-velocity zone at the transition depth of 173 ft (53 m) in profile P2, the increase in the scale factor was applied at a depth of 276 ft (84 m), coincident with an increase in the mean base-case profile (elevation -317 ft in Table 2.3.1-1). The scale factors of 1.25 and 1.57 reflect a $\sigma_{\mu ln}$ of about 0.2 and about 0.35 respectively based on the SPID (EPRI, 2013a) 10th and 90th fractiles which implies a scale factor of 1.28 on $\sigma_{\mu ln}$. Depth to Precambrian basement was taken at 4,000 ft (1,219 m) randomized $\pm 1,200$ ft (366 m). The three shear-wave velocity profiles are shown in Figure 2.3.2-1 and listed in Table 2.3.2-1. (EPRI, 2014)

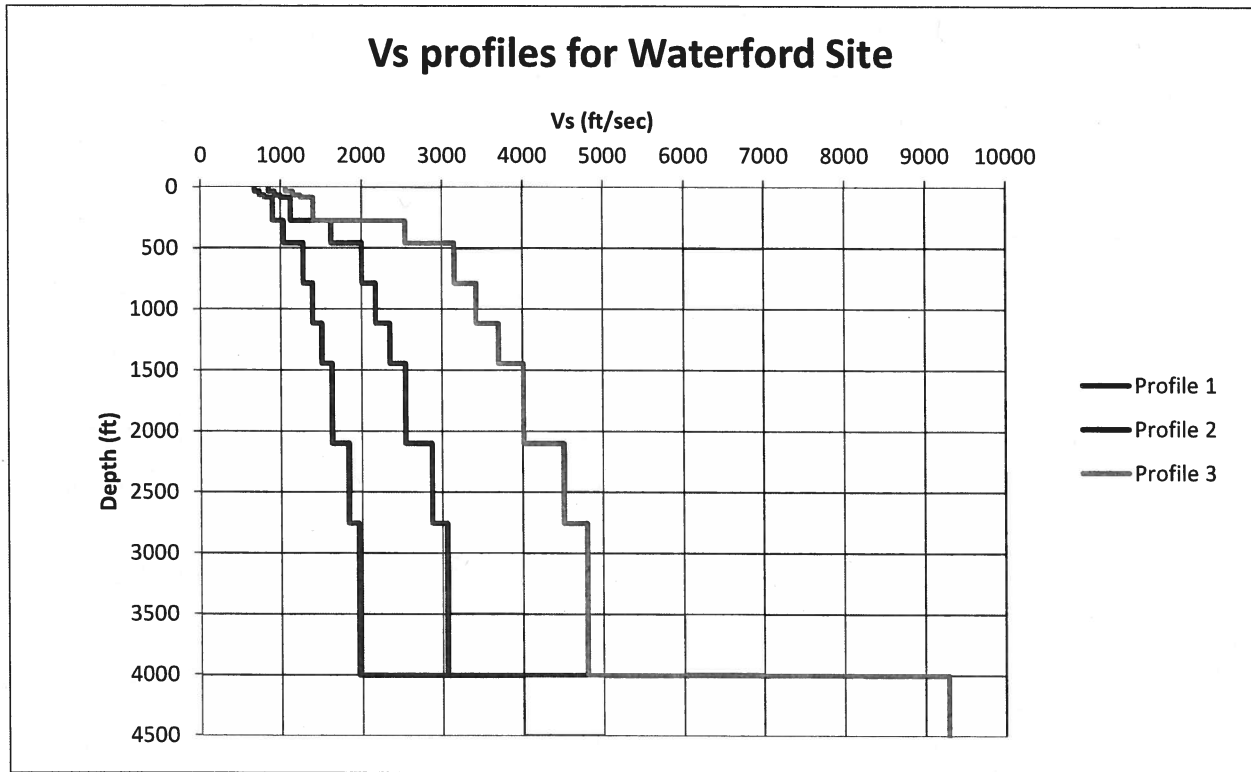


Figure 2.3.2-1. Shear-wave velocity profiles for WSES-3. (EPRI, 2014)

Table 2.3.2-1. Layer thicknesses, depths, and shear-wave velocities (Vs) for 3 profiles, WSES-3. (EPRI, 2014)

| Profile 1 | | | Profile 2 | | | Profile 3 | | |
|----------------|------------|-----------|----------------|------------|-----------|----------------|------------|-----------|
| thickness (ft) | depth (ft) | Vs (ft/s) | thickness (ft) | depth (ft) | Vs (ft/s) | thickness (ft) | depth (ft) | Vs (ft/s) |
| | 0 | 850 | | 0 | 680 | | 0 | 1062 |
| 9.2 | 9.2 | 850 | 9.2 | 9.2 | 680 | 9.2 | 9.2 | 1062 |
| 9.2 | 18.5 | 850 | 9.2 | 18.5 | 680 | 9.2 | 18.5 | 1062 |
| 1.5 | 20.0 | 850 | 1.5 | 20.0 | 680 | 1.5 | 20.0 | 1062 |
| 8.5 | 28.5 | 850 | 8.5 | 28.5 | 680 | 8.5 | 28.5 | 1062 |
| 8.5 | 37.0 | 850 | 8.5 | 37.0 | 680 | 8.5 | 37.0 | 1062 |
| 7.5 | 44.5 | 925 | 7.5 | 44.5 | 740 | 7.5 | 44.5 | 1156 |
| 7.5 | 52.0 | 925 | 7.5 | 52.0 | 740 | 7.5 | 52.0 | 1156 |
| 8.0 | 60.0 | 925 | 8.0 | 60.0 | 740 | 8.0 | 60.0 | 1156 |
| 8.0 | 68.0 | 925 | 8.0 | 68.0 | 740 | 8.0 | 68.0 | 1156 |
| 8.0 | 76.0 | 1000 | 8.0 | 76.0 | 800 | 8.0 | 76.0 | 1250 |
| 11.0 | 87.0 | 1000 | 11.0 | 87.0 | 800 | 11.0 | 87.0 | 1250 |
| 12.7 | 99.7 | 1125 | 12.7 | 99.7 | 900 | 12.7 | 99.7 | 1406 |
| 12.7 | 112.3 | 1125 | 12.7 | 112.3 | 900 | 12.7 | 112.3 | 1406 |
| 7.7 | 120.0 | 1125 | 7.7 | 120.0 | 900 | 7.7 | 120.0 | 1406 |
| 8.8 | 128.8 | 1125 | 8.8 | 128.8 | 900 | 8.8 | 128.8 | 1406 |
| 8.8 | 137.7 | 1125 | 8.8 | 137.7 | 900 | 8.8 | 137.7 | 1406 |

Table 2.3.2-1. Layer thicknesses, depths, and shear-wave velocities (Vs) for 3 profiles, WSES-3. (EPRI, 2014)

| Profile 1 | | | Profile 2 | | | Profile 3 | | |
|-------------------|---------------|--------------|-------------------|---------------|--------------|-------------------|---------------|--------------|
| thickness (ft) | depth (ft) | Vs (ft/s) | thickness (ft) | depth (ft) | Vs (ft/s) | thickness (ft) | depth (ft) | Vs (ft/s) |
| 12.7 | 150.3 | 1125 | 12.7 | 150.3 | 900 | 12.7 | 150.3 | 1406 |
| 12.7 | 163.0 | 1125 | 12.7 | 163.0 | 900 | 12.7 | 163.0 | 1406 |
| 12.7 | 175.7 | 1125 | 12.7 | 175.7 | 900 | 12.7 | 175.7 | 1406 |
| 12.7 | 188.3 | 1125 | 12.7 | 188.3 | 900 | 12.7 | 188.3 | 1406 |
| 12.7 | 201.0 | 1125 | 12.7 | 201.0 | 900 | 12.7 | 201.0 | 1406 |
| 12.7 | 213.7 | 1125 | 12.7 | 213.7 | 900 | 12.7 | 213.7 | 1406 |
| 12.7 | 226.3 | 1125 | 12.7 | 226.3 | 900 | 12.7 | 226.3 | 1406 |
| 12.7 | 239.0 | 1125 | 12.7 | 239.0 | 900 | 12.7 | 239.0 | 1406 |
| 12.7 | 251.7 | 1125 | 12.7 | 251.7 | 900 | 12.7 | 251.7 | 1406 |
| 12.7 | 264.3 | 1125 | 12.7 | 264.3 | 900 | 12.7 | 264.3 | 1406 |
| 12.7 | 277.0 | 1125 | 12.7 | 277.0 | 900 | 12.7 | 277.0 | 1406 |
| 18.3 | 295.3 | 1625 | 18.3 | 295.3 | 1040 | 18.3 | 295.3 | 2551 |
| 18.3 | 313.6 | 1625 | 18.3 | 313.6 | 1040 | 18.3 | 313.6 | 2551 |
| 18.3 | 331.9 | 1625 | 18.3 | 331.9 | 1040 | 18.3 | 331.9 | 2551 |
| 18.3 | 350.2 | 1625 | 18.3 | 350.2 | 1040 | 18.3 | 350.2 | 2551 |
| 18.3 | 368.5 | 1625 | 18.3 | 368.5 | 1040 | 18.3 | 368.5 | 2551 |
| 18.3 | 386.8 | 1625 | 18.3 | 386.8 | 1040 | 18.3 | 386.8 | 2551 |
| 18.3 | 405.1 | 1625 | 18.3 | 405.1 | 1040 | 18.3 | 405.1 | 2551 |
| 18.3 | 423.4 | 1625 | 18.3 | 423.4 | 1040 | 18.3 | 423.4 | 2551 |
| 18.3 | 441.7 | 1625 | 18.3 | 441.7 | 1040 | 18.3 | 441.7 | 2551 |
| 18.3 | 460.0 | 1625 | 18.3 | 460.0 | 1040 | 18.3 | 460.0 | 2551 |
| 40.0 | 500.0 | 2005 | 40.0 | 500.0 | 1283 | 40.0 | 500.0 | 3147 |
| 40.0 | 540.1 | 2005 | 40.0 | 540.1 | 1283 | 40.0 | 540.1 | 3147 |
| 40.0 | 580.1 | 2005 | 40.0 | 580.1 | 1283 | 40.0 | 580.1 | 3147 |
| 40.0 | 620.1 | 2005 | 40.0 | 620.1 | 1283 | 40.0 | 620.1 | 3147 |
| 40.0 | 660.1 | 2005 | 40.0 | 660.1 | 1283 | 40.0 | 660.1 | 3147 |
| 42.7 | 702.8 | 2005 | 42.7 | 702.8 | 1283 | 42.7 | 702.8 | 3147 |
| 42.7 | 745.4 | 2005 | 42.7 | 745.4 | 1283 | 42.7 | 745.4 | 3147 |
| 42.7 | 788.1 | 2005 | 42.7 | 788.1 | 1283 | 42.7 | 788.1 | 3147 |
| 65.6 | 853.7 | 2182 | 65.6 | 853.7 | 1396 | 65.6 | 853.7 | 3425 |
| 65.6 | 919.3 | 2182 | 65.6 | 919.3 | 1396 | 65.6 | 919.3 | 3425 |
| 65.6 | 984.9 | 2182 | 65.6 | 984.9 | 1396 | 65.6 | 984.9 | 3425 |
| 65.6 | 1050.6 | 2182 | 65.6 | 1050.6 | 1396 | 65.6 | 1050.6 | 3425 |
| 65.6 | 1116.2 | 2182 | 65.6 | 1116.2 | 1396 | 65.6 | 1116.2 | 3425 |
| 65.6 | 1181.8 | 2359 | 65.6 | 1181.8 | 1510 | 65.6 | 1181.8 | 3704 |
| 65.6 | 1247.4 | 2359 | 65.6 | 1247.4 | 1510 | 65.6 | 1247.4 | 3704 |
| 65.6 | 1313.0 | 2359 | 65.6 | 1313.0 | 1510 | 65.6 | 1313.0 | 3704 |
| 65.6 | 1378.6 | 2359 | 65.6 | 1378.6 | 1510 | 65.6 | 1378.6 | 3704 |
| 65.6 | 1444.3 | 2359 | 65.6 | 1444.3 | 1510 | 65.6 | 1444.3 | 3704 |

Table 2.3.2-1. Layer thicknesses, depths, and shear-wave velocities (V_s) for 3 profiles, WSES-3. (EPRI, 2014)

| Profile 1 | | | Profile 2 | | | Profile 3 | | |
|----------------|------------|--------------|----------------|------------|--------------|----------------|------------|--------------|
| thickness (ft) | depth (ft) | V_s (ft/s) | thickness (ft) | depth (ft) | V_s (ft/s) | thickness (ft) | depth (ft) | V_s (ft/s) |
| 131.2 | 1575.5 | 2552 | 131.2 | 1575.5 | 1634 | 131.2 | 1575.5 | 4007 |
| 131.2 | 1706.7 | 2552 | 131.2 | 1706.7 | 1634 | 131.2 | 1706.7 | 4007 |
| 131.2 | 1838.0 | 2552 | 131.2 | 1838.0 | 1634 | 131.2 | 1838.0 | 4007 |
| 131.2 | 1969.2 | 2552 | 131.2 | 1969.2 | 1634 | 131.2 | 1969.2 | 4007 |
| 131.2 | 2100.4 | 2552 | 131.2 | 2100.4 | 1634 | 131.2 | 2100.4 | 4007 |
| 131.2 | 2231.7 | 2871 | 131.2 | 2231.7 | 1837 | 131.2 | 2231.7 | 4507 |
| 131.2 | 2362.9 | 2871 | 131.2 | 2362.9 | 1837 | 131.2 | 2362.9 | 4507 |
| 131.2 | 2494.1 | 2871 | 131.2 | 2494.1 | 1837 | 131.2 | 2494.1 | 4507 |
| 131.2 | 2625.4 | 2871 | 131.2 | 2625.4 | 1837 | 131.2 | 2625.4 | 4507 |
| 131.2 | 2756.6 | 2871 | 131.2 | 2756.6 | 1837 | 131.2 | 2756.6 | 4507 |
| 1246.5 | 4003.1 | 3054 | 1246.5 | 4003.1 | 1955 | 1246.5 | 4003.1 | 4795 |
| 3280.8 | 7283.9 | 9285 | 3280.8 | 7283.9 | 9285 | 3280.8 | 7283.9 | 9285 |

2.3.2.1 Shear Modulus and Damping Curves

Site-specific nonlinear dynamic material properties were not available for WSES-3 soils. The soil material over the upper 500 ft (150 m) was assumed to have behavior that could be modeled with either EPRI cohesionless soil or Peninsular Range (PR) G/G_{max} and hysteretic damping curves (EPRI, 2013a). Consistent with the SPID (EPRI, 2013a), the EPRI soil curves (model M1) were considered to be appropriate to represent the more nonlinear response likely to occur in the materials at this site. The PR curves (EPRI, 2013a) for soils (model M2) was assumed to represent an equally plausible alternative more linear response across loading level. (EPRI, 2014)

2.3.2.2 Kappa

Base-case kappa estimates were determined using Section B-5.1.3.1 of the SPID (EPRI, 2013a) for a deep greater than 3000 ft (1000 m) CEUS soil site. Kappa for a soil site with greater than 3,000 ft (1 km) is assumed to have the maximum kappa value of 0.04 s (Table 2.3.2-2). Epistemic uncertainty in profile damping (kappa) was considered to be accommodated at design loading levels by the multiple (2) sets of G/G_{max} and hysteretic damping curves. (EPRI, 2014)

Table 2.3.2-2. Kappa Values and Weights Used for Site Response Analyses. (EPRI, 2014)

| | |
|--|----------|
| Velocity Profile | Kappa(s) |
| P1 | 0.040 |
| P2 | 0.040 |
| P3 | 0.040 |
| | |
| Velocity Profile | Weights |
| P1 | 0.4 |
| P2 | 0.3 |
| P3 | 0.3 |
| | |
| G/G _{max} and Hysteretic Damping Curves | |
| M1 | 0.5 |
| M2 | 0.5 |

2.3.3 Randomization of Base Case Profiles

To account for the aleatory variability in dynamic material properties that is expected to occur across a site at the scale of a typical nuclear facility, variability in the assumed shear-wave velocity profiles has been incorporated in the site response calculations. For WSES-3 random shear wave velocity profiles were developed from the base case profiles shown in Figure 2.3.2-1. Consistent with the discussion in Appendix B of the SPID (EPRI, 2013a), the velocity randomization procedure made use of random field models which describe the statistical correlation between layering and shear wave velocity. The default randomization parameters developed in (Toro, 1997) for United States Geological Survey “A” site conditions were used for this site. Thirty random velocity profiles were generated for each base case profile. These random velocity profiles were generated using a natural log standard deviation of 0.25 over the upper 50 ft and 0.15 below that depth. As specified in the SPID (EPRI, 2013a), correlation of shear wave velocity between layers was modeled using the footprint correlation model. In the correlation model, a limit of ± 2 standard deviations about the median value in each layer was assumed for the limits on random velocity fluctuations. (EPRI, 2014)

2.3.4 Input Spectra

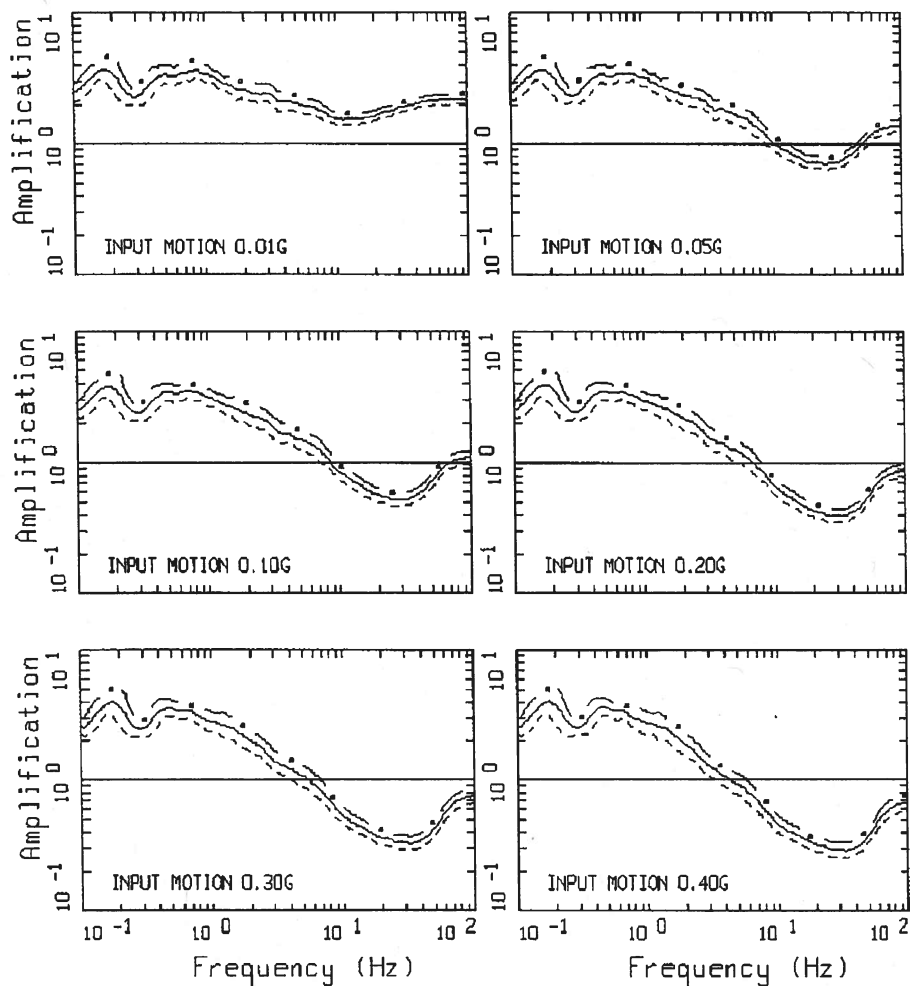
Consistent with the guidance in Appendix B of the SPID (EPRI, 2013a), input Fourier amplitude spectra were defined for a single representative earthquake magnitude (**M** 6.5) using two different assumptions regarding the shape of the seismic source spectrum (single-corner and double-corner). A range of 11 different input amplitudes (median Peak Ground Accelerations (PGAs) ranging from 0.01 to 1.5g) were used in the site response analyses. The characteristics of the seismic source and upper crustal attenuation properties assumed for the analysis of the WSES-3 were the same as those identified in Tables B-4, B-5, B-6 and B-7 of the SPID (EPRI, 2013a) as appropriate for typical CEUS sites. (EPRI, 2014)

2.3.5 Methodology

To perform the site response analyses for WSES-3, a random vibration theory approach was employed. This process utilizes a simple, efficient approach for computing site-specific amplification functions and is consistent with existing NRC guidance and the SPID (EPRI, 2013a). The guidance contained in Appendix B of the SPID (EPRI, 2013a) on incorporating epistemic uncertainty in shear-wave velocities, kappa, non-linear dynamic properties and source spectra for plants with limited at-site information was followed for WSES-3. (EPRI, 2014)

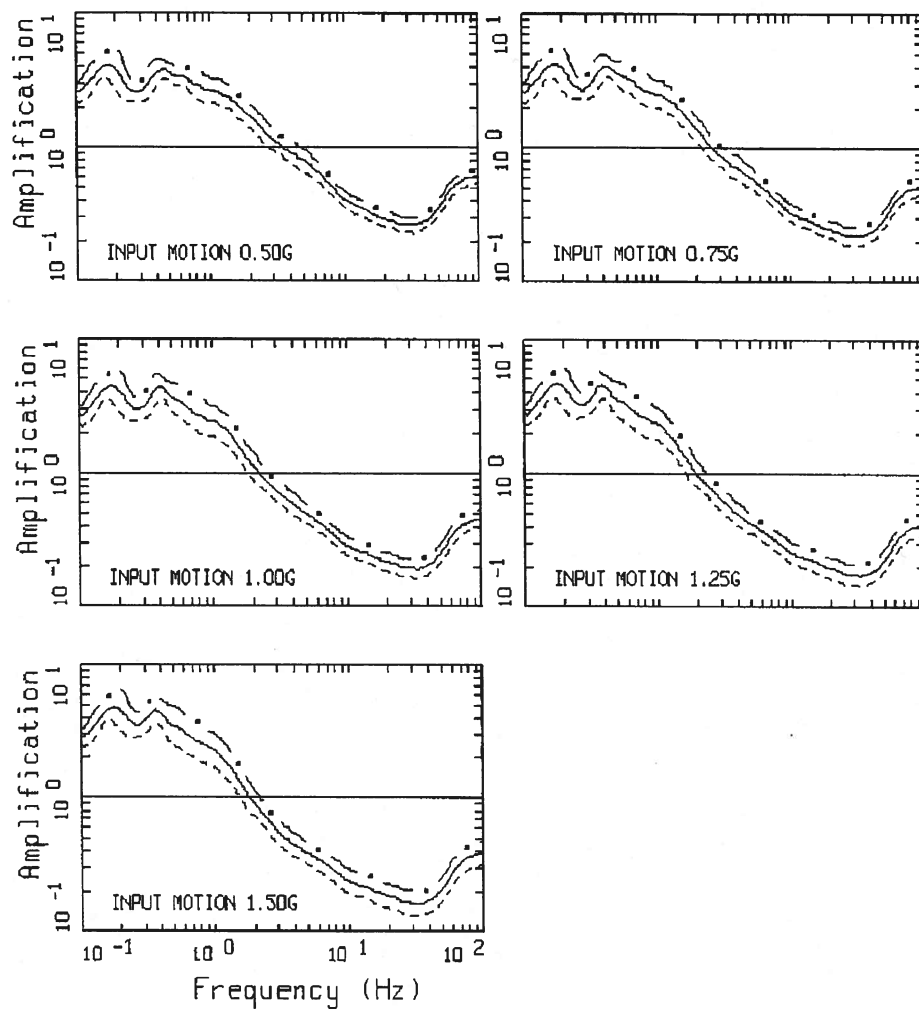
2.3.6 Amplification Functions

The results of the site response analysis consist of amplification factors (5% damped pseudo absolute response spectra) which describe the amplification (or de-amplification) of hard reference rock motion as a function of frequency and input reference rock amplitude. The amplification factors are represented in terms of a median amplification value and an associated standard deviation (σ) for each oscillator frequency and input rock amplitude. Consistent with the SPID (EPRI, 2013a) a minimum median amplification value of 0.5 was employed in the present analysis. Figure 2.3.6-1 illustrates the median and ± 1 standard deviation in the predicted amplification factors developed for the eleven loading levels parameterized by the median reference (hard rock) peak acceleration (0.01g to 1.50g) for profile P1 and EPRI soil G/G_{\max} and hysteretic damping curves (EPRI, 2013a). The variability in the amplification factors results from variability in shear-wave velocity, depth to hard rock, and modulus reduction and hysteretic damping curves. To illustrate the effects of more linear response at WSES-3 deep soil site, Figure 2.3.6-2 shows the corresponding amplification factors developed with PR curves for soil (model M2). Between the more nonlinear and more linear analyses, Figures 2.3.6-1 and Figure 2.3.6-2 respectively show little difference below about 10 Hz across loading level. Tabular data for Figures 2.3.6-1 and Figure 2.3.6-2 is provided For Information Only in Appendix A. (EPRI, 2014)



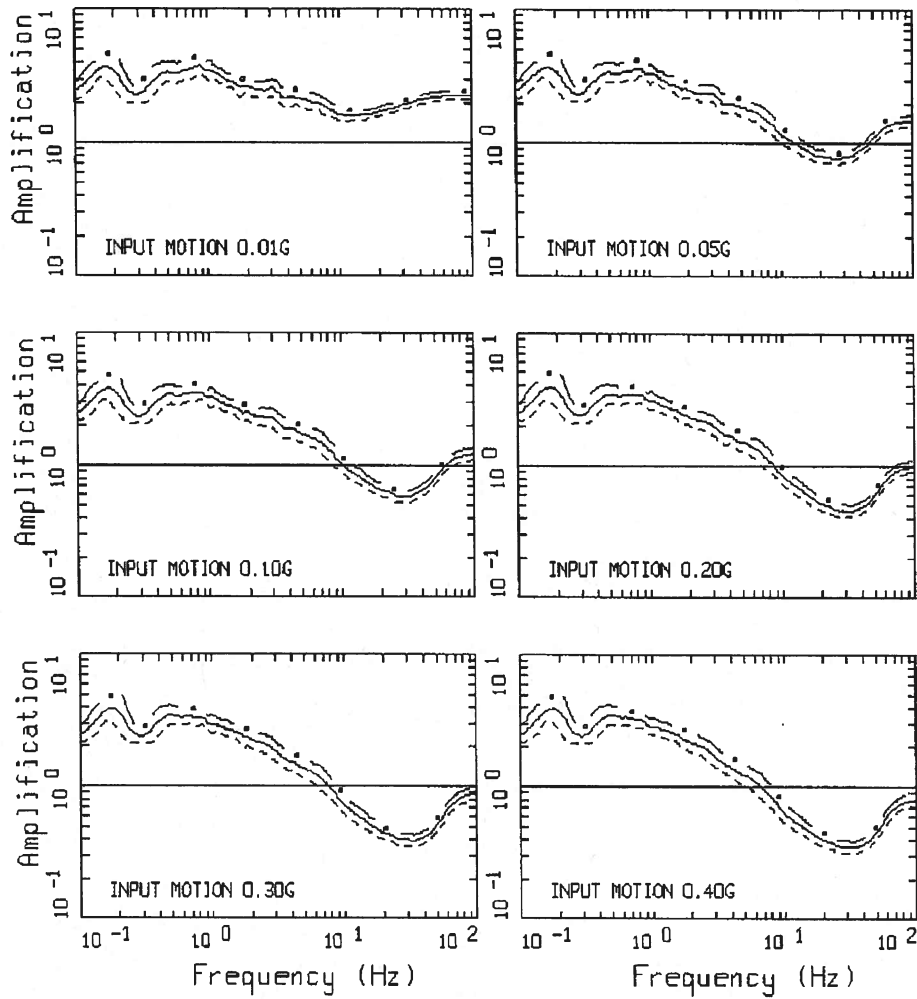
AMPLIFICATION, WATERFORD, M1P1K1
M 6.5, 1 CORNER: PAGE 1 OF 2

Figure 2.3.6-1. Example suite of amplification factors (5% damping pseudo absolute acceleration spectra) developed for the mean base-case profile (P1), EPRI soil modulus reduction and hysteretic damping curves (model M1), and base-case kappa (K1) at eleven loading levels of hard rock median peak acceleration values from 0.01g to 1.50g. M 6.5 and single-corner source model (EPRI, 2013a). (EPRI, 2014)



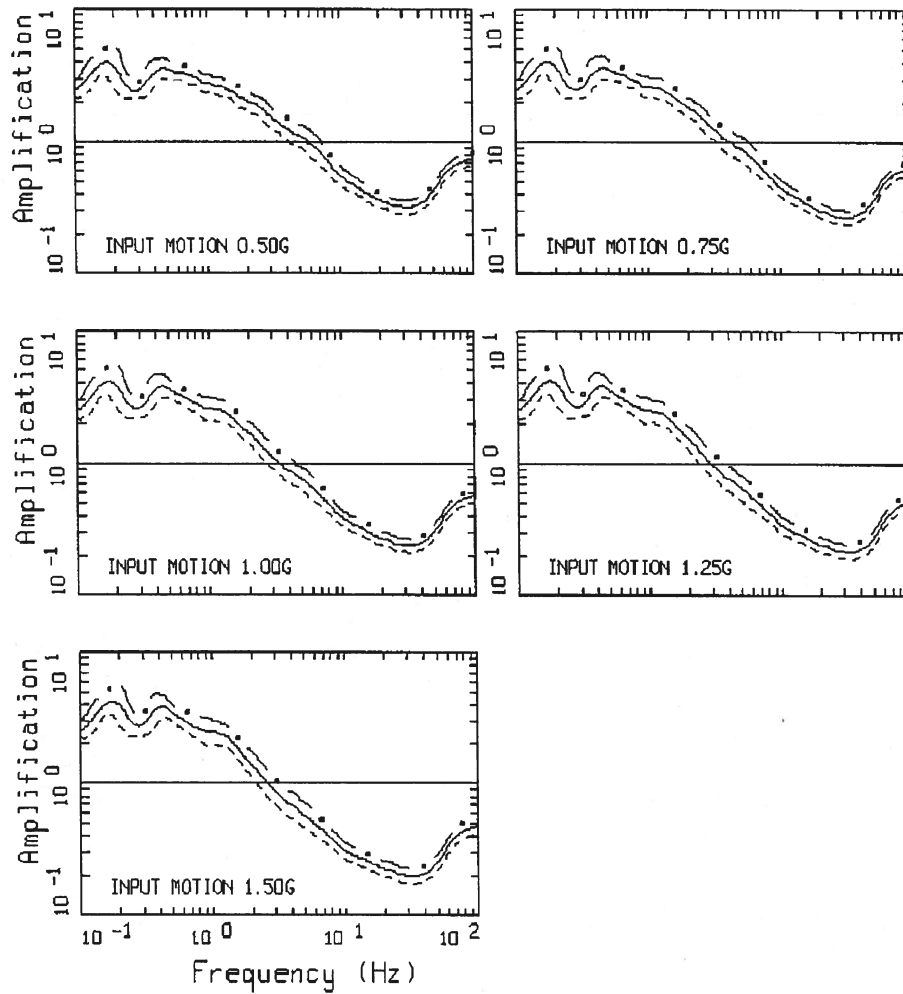
AMPLIFICATION, WATERFORD, M1P1K1
M 6.5, 1 CORNER: PAGE 2 OF 2

Figure 2.3.6-1.(cont.)



AMPLIFICATION, WATERFORD, M2P1K1
M 6.5, 1 CORNER: PAGE 1 OF 2

Figure 2.3.6-2. Example suite of amplification factors (5% damping pseudo absolute acceleration spectra) developed for the mean base-case profile (P1), Peninsular Range curves for soil (model M2), and base-case kappa (K1) at eleven loading levels of hard rock median peak acceleration values from 0.01g to 1.50g. M 6.5 and single-corner source model (EPRI, 2013a). (EPRI, 2014)



AMPLIFICATION, WATERFORD, M2P1K1
M 6.5, 1 CORNER: PAGE 2 OF 2

Figure 2.3.6-2.(cont.)

2.3.7 Control Point Seismic Hazard Curves

The procedure to develop probabilistic site-specific control point hazard curves used in the present analysis follows the methodology described in Section B-6.0 of the SPID (EPRI, 2013a). This procedure (referred to as Method 3) computes a site-specific control point hazard curve for a broad range of spectral accelerations given the site-specific bedrock hazard curve and site-specific estimates of soil or soft-rock response and associated uncertainties. This process is repeated for each of the seven spectral frequencies for which ground motion equations are available. The dynamic response of the materials below the control point was represented by the frequency- and amplitude-dependent amplification functions (median values and standard deviations) developed and described in the previous section. The resulting control point mean hazard curves for WSES-3 are shown in Figure 2.3.7-1 for the seven spectral frequencies for which ground motion equations are defined. Tabulated values of mean and fractile seismic hazard curves and site response amplification functions are provided in Appendix A. (EPRI, 2014)

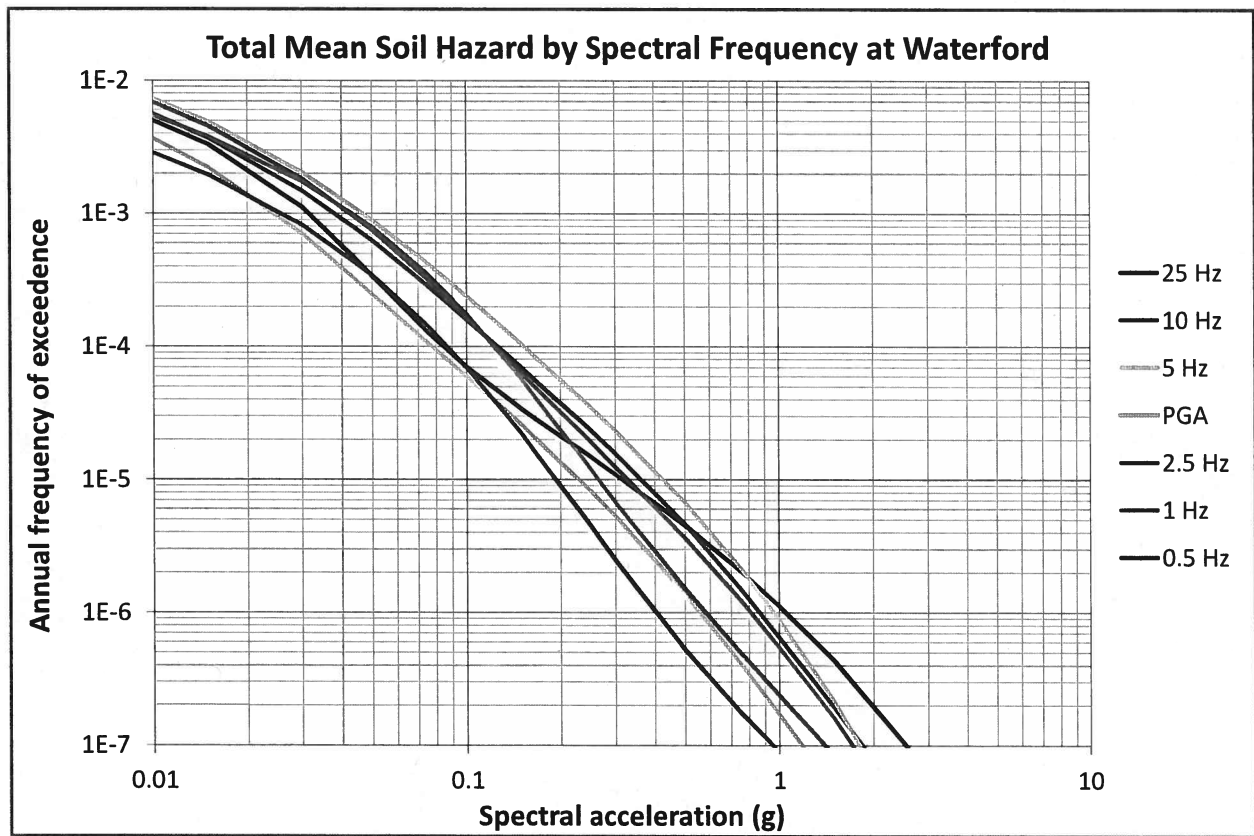


Figure 2.3.7-1. Control point mean hazard curves for spectral frequencies of 0.5, 1.0, 2.5, 5.0, 10, 25 and PGA (100) Hz at WSES-3. (EPRI, 2014)

2.4 Control Point Response Spectrum

The control point hazard curves described above have been used to develop Uniform Hazard Response Spectra (UHRS) and the GMRS. The UHRS were obtained through linear interpolation in log-log space to estimate the spectral acceleration at each spectral frequency for the 10^{-4} and 10^{-5} per year hazard levels. Table 2.4-1 shows the UHRS and GMRS accelerations for a range of frequencies. (EPRI, 2014)

Table 2.4-1. UHRS and GMRS for WSES-3. (EPRI, 2014)

| Frequency(Hz) | 10^{-4} UHRS (g) | 10^{-5} UHRS (g) | GMRS (g) |
|---------------|-----------------------|-----------------------|-------------|
| 100 | 7.75E-02 | 2.27E-01 | 1.10E-01 |
| 90 | 7.75E-02 | 2.32E-01 | 1.12E-01 |
| 80 | 7.76E-02 | 2.37E-01 | 1.14E-01 |
| 70 | 7.77E-02 | 2.44E-01 | 1.16E-01 |
| 60 | 7.80E-02 | 2.51E-01 | 1.19E-01 |
| 50 | 7.83E-02 | 2.61E-01 | 1.23E-01 |
| 40 | 7.91E-02 | 2.74E-01 | 1.28E-01 |
| 35 | 7.99E-02 | 2.84E-01 | 1.32E-01 |
| 30 | 8.14E-02 | 2.96E-01 | 1.37E-01 |
| 25 | 8.44E-02 | 3.15E-01 | 1.45E-01 |
| 20 | 8.88E-02 | 3.12E-01 | 1.45E-01 |
| 15 | 9.94E-02 | 3.20E-01 | 1.52E-01 |
| 12.5 | 1.10E-01 | 3.36E-01 | 1.61E-01 |
| 10 | 1.25E-01 | 3.61E-01 | 1.75E-01 |
| 9 | 1.31E-01 | 3.77E-01 | 1.83E-01 |
| 8 | 1.37E-01 | 3.92E-01 | 1.91E-01 |
| 7 | 1.42E-01 | 3.99E-01 | 1.95E-01 |
| 6 | 1.50E-01 | 4.13E-01 | 2.02E-01 |
| 5 | 1.53E-01 | 4.23E-01 | 2.07E-01 |
| 4 | 1.50E-01 | 4.06E-01 | 2.00E-01 |
| 3.5 | 1.47E-01 | 3.89E-01 | 1.92E-01 |
| 3 | 1.42E-01 | 3.70E-01 | 1.83E-01 |
| 2.5 | 1.23E-01 | 3.28E-01 | 1.62E-01 |
| 2 | 1.25E-01 | 3.10E-01 | 1.55E-01 |
| 1.5 | 1.27E-01 | 2.99E-01 | 1.51E-01 |
| 1.25 | 1.25E-01 | 2.83E-01 | 1.44E-01 |
| 1 | 1.22E-01 | 2.64E-01 | 1.36E-01 |
| 0.9 | 1.20E-01 | 2.60E-01 | 1.34E-01 |
| 0.8 | 1.16E-01 | 2.53E-01 | 1.30E-01 |
| 0.7 | 1.07E-01 | 2.38E-01 | 1.22E-01 |
| 0.6 | 9.75E-02 | 2.14E-01 | 1.10E-01 |
| 0.5 | 8.64E-02 | 1.92E-01 | 9.84E-02 |

Table 2.4-1. UHRS and GMRS for WSES-3. (EPRI, 2014)

| Frequency(Hz) | 10^{-4} UHRS (g) | 10^{-5} UHRS (g) | GMRS (g) |
|---------------|--------------------|--------------------|----------|
| 0.4 | 6.91E-02 | 1.54E-01 | 7.87E-02 |
| 0.35 | 6.05E-02 | 1.35E-01 | 6.89E-02 |
| 0.3 | 5.18E-02 | 1.15E-01 | 5.90E-02 |
| 0.25 | 4.32E-02 | 9.62E-02 | 4.92E-02 |
| 0.2 | 3.46E-02 | 7.70E-02 | 3.93E-02 |
| 0.15 | 2.59E-02 | 5.77E-02 | 2.95E-02 |
| 0.125 | 2.16E-02 | 4.81E-02 | 2.46E-02 |
| 0.1 | 1.73E-02 | 3.85E-02 | 1.97E-02 |

The 10^{-4} and 10^{-5} UHRS are used to compute the GMRS at the control point and are shown in Figure 2.4-1.

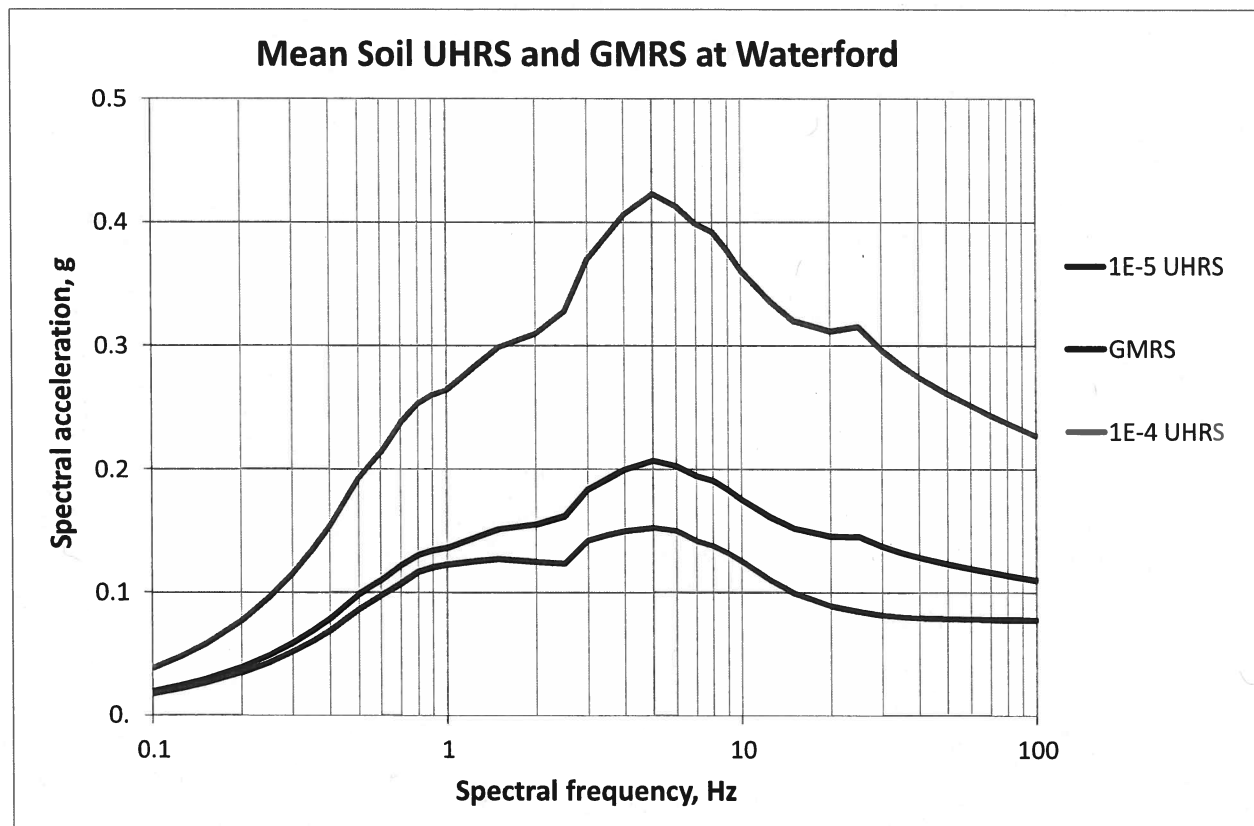


Figure 2.4-1. UHRS for 10^{-4} and 10^{-5} and GMRS at control point for WSES-3 (5%-damped response spectra). (EPRI, 2014)

3.0 Plant Design Basis and Beyond Design Basis Evaluation Ground Motion

The design basis for WSES-3 is identified in the Final Safety Analysis Report (Entergy, 2013) and other pertinent documents.

3.1 SSE Description of Spectral Shape

The SSE for WSES-3 was set at the legal minimum specified by 10 CFR Part 100, Appendix A. This very conservative surface acceleration is double the maximum acceleration appropriate for the maximum earthquake which has occurred in the site's tectonic province during the past 250 years. (Entergy, 2013)

The SSE is defined in terms of a PGA and a design response spectrum. Table 3.1-1 shows the Spectral Acceleration (SA) values as a function of frequency for the 5% damped horizontal SSE. (EPRI, 2014)

Table 3.1-1. SSE for WSES-3 (Entergy, 2013)

| | | | | |
|----------------|-----|------|------|------|
| Frequency (Hz) | 25 | 5.6 | 2 | 0.33 |
| SA (g) | 0.1 | 0.25 | 0.25 | 0.04 |

In order to better define the SSE spectrum over the frequency range of interest, additional spectral acceleration points were developed based on the 5% design basis earthquake plot shown in the WSES-3 FSAR Figure 3.7-2 (Entergy, 2013). It was also observed that the entire nuclear island at WSES-3, including all safety related Structures, Systems, and Components (SSC), was analyzed in a Soil Structure Interaction Analysis (SSIA) represented as a mat on springs using a time history having spectral accelerations that enveloped the SSE spectrum. In accordance with design basis documents, SSIA were also conducted via Stardyne 3 analyses that modeled the mat and side walls of the nuclear island and also derived vertical and lateral soil pressure. The initial model used for the SSIA is shown in the WSES-3 FSAR Figure 3.7-9 (Entergy, 2013).

The response spectrum of the time history used to represent the SSE, or design basis earthquake, for the SSIA envelopes the SSE spectrum, as shown in the WSES-3 FSAR Figure 3.7-2 (Entergy, 2013). The spectral accelerations of the SSE Time History (T/H) spectrum for 5% damping are also tabulated in Table 3.1-2.

Table 3.1-2. Revised SSE Tabulation for WSES-3

| Period (Sec) | Frequency (Hz) | SSE Spectrum Acc. (g) | SSE Time History Spectrum Acc. (g) |
|--------------|----------------|-----------------------|------------------------------------|
| 0.01 | 100.00 | 0.1 | 0.135 |
| 0.04 | 25.00 | 0.125 | 0.135 |
| 0.1 | 10.00 | 0.175 | 0.23 |
| 0.2 | 5.00 | 0.245 | 0.3 |
| 0.4 | 2.50 | 0.245 | 0.32 |
| 0.5 | 2.00 | 0.245 | 0.28 |
| 0.67 | 1.50 | 0.19 | 0.24 |
| 0.8 | 1.35 | 0.18 | 0.235 |
| 0.9 | 1.10 | 0.135 | 0.17 |
| 1.0 | 1.00 | 0.12 | 0.155 |
| 2.0 | 0.50 | 0.062 | 0.088 |

3.2 Control Point Elevation

The entire WSES-3 nuclear island is supported on a common mat. As shown in the WSES-3 FSAR Figure 3.7-9 (Entergy, 2013), the bottom of the mat is at elevation -47 ft MSL. Therefore, the SSE control point elevation is defined at elevation -47 ft MSL.

3.3 IPEEE Description and Capacity Response Spectrum

The Individual Plant Examination of External Events (IPEEE) was performed as a reduced scope. As discussed below, WSES-3 screens-out from performing further risk evaluations. Therefore, the IPEEE was not reviewed.

4.0 Screening Evaluation

In accordance with SPID Section 3 (EPRI, 2013a), a screening evaluation was performed as described below.

4.1 Risk Evaluation Screening (1 to 10 Hz)

In the 1 to 10 Hz part of the response spectrum, the SSE exceeds the GMRS when using the reduced number of frequency points shown in Table 3.1-1. However, when the revised SSE tabulation shown in Table 3.1-2 is used, there is an approximately 10% or less exceedance of the SSE spectral values by the GMRS around 1.0 Hz. In accordance with Section 3.2.1.1 of the SPID (EPRI, 2013a), for the low seismic hazard WSES-3 site, it would be necessary to identify all safety related SSCs that may be susceptible to damage from the GMRS accelerations at the

point where they exceed the SSE accelerations, and then derive High Confidence in Low Probability of Failure (HCLPF) estimates for these components based on the GMRS to show that the HCLPF is greater than the GMRS.

In lieu of identifying susceptible SSCs and developing HCLPF estimates, it is noted that all safety-related SSCs were designed based on responses obtained using an SSE time history that has a spectrum that envelopes the GMRS over the entire 1 Hz to 10 Hz range.

Furthermore, all design work using floor response spectra derived from the time history Soil Structure Interaction Analyses (SSIA) conservatively assumed the spectral peak at about 1.66 Hz or higher extends over the lower frequency range, as shown in FSAR Figures 3.7-11 through 3.7-20 (Entergy, 2013). Thus, the response spectra derived from a time history analysis, with the time history having a spectrum that envelopes the GMRS in the 1 Hz to 10 Hz range, were conservatively used via a design envelope that extended the 1.66 Hz or higher spectra peaks to frequencies less than 1.66 Hz. As such, it is demonstrated that all safety related SSCs were designed for seismic accelerations higher than the GMRS accelerations in the 1 Hz to 10 Hz part of the response spectrum.

Therefore, no further risk evaluation will be performed.

Additionally, based on the SSE and GMRS comparison, WSES-3 will screen-out of the expedited seismic evaluation described in EPRI 3002000704 (EPRI, 2013b) as proposed in a letter to the NRC (ML13101A379) dated April 9, 2013 (NEI, 2013) and agreed to by the NRC (ML13106A331) in a letter dated May 7, 2013 (U.S. NRC, 2013).

4.2 High Frequency Screening (> 10 Hz)

For a portion of the range above 10 Hz, the 5% damping GMRS exceeds the 5% damping SSE spectrum by less than 15%. The maximum accelerations in the GMRS exceedance range are 0.15g or less. Furthermore, the 5% damping spectrum of the time history used to derive seismic responses for all safety related SSCs is within less than 8% of the GMRS accelerations in the exceedance range. It is also noted that the WSES-3 soil-spring system has a natural frequency in the 1.5 Hz range, with the highest mode participating in the response being at 10 Hz or less. As shown in the WSES-3 FSAR (Entergy, 2013) Figures 3.7-11 through 3.7-20, the floor response spectra become quasi-steady state above 10 Hz. Thus, the seismic high frequency content is filtered out by the soil-structure system.

Considering the very low accelerations in the high frequency range, the fact that high frequency susceptible components were designed/assessed for acceleration levels within 8% of the GMRS accelerations in the high frequency range and frequency content above 10 Hz is filtered out by the soil-structure system, no further considerations are considered to be required. Therefore, a High Frequency Confirmation will not be performed.

4.3 Spent Fuel Pool Evaluation Screening (1 to 10 Hz)

In the 1 to 10 Hz part of the response spectrum, the SSE exceeds the GMRS. Therefore, a Spent Fuel Pool evaluation will not be performed.

5.0 Interim Actions

Based on the screening evaluation, the expedited seismic evaluation described in EPRI 3002000704 (EPRI, 2013b) will not be performed.

Consistent with NRC letter (ML14030A046) dated February 20, 2014 (U.S. NRC, 2014), the seismic hazard reevaluations presented herein are distinct from the current design and licensing bases of WSES-3. Therefore, the results do not call into question the operability or functionality of SSCs and are not reportable pursuant to 10 CFR 50.72, "Immediate notification requirements for operating nuclear power reactors," and 10 CFR 50.73, "Licensee event report system."

The NRC letter also requests that licensees provide an interim evaluation or actions to demonstrate that the plant can cope with the reevaluated hazard while the expedited approach and risk evaluations are conducted. In response to that request, NEI letter dated March 12, 2014 (NEI, 2014), provides seismic core damage risk estimates using the updated seismic hazards for the operating nuclear plants in the Central and Eastern United States. These risk estimates continue to support the following conclusions of the NRC GI-199 Safety/Risk Assessment (U.S. NRC, 2010):

Overall seismic core damage risk estimates are consistent with the Commission's Safety Goal Policy Statement because they are within the subsidiary objective of 10^{-4} /year for core damage frequency. The GI-199 Safety/Risk Assessment, based in part on information from the U.S. Nuclear Regulatory Commission's (NRC's) Individual Plant Examination of External Events (IPEEE) program, indicates that no concern exists regarding adequate protection and that the current seismic design of operating reactors provides a safety margin to withstand potential earthquakes exceeding the original design basis.

WSES-3 is included in the March 12, 2014 risk estimates (NEI, 2014). Using the methodology described in the NEI letter, all plants were shown to be below 10^{-4} /year; thus, the above conclusions apply.

In accordance with the Near-Term Task Force Recommendation 2.3, WSES-3 performed seismic walkdowns using the guidance in EPRI Report 1025286 (EPRI, 2012). The seismic walkdowns were completed and captured in Fukushima Seismic Walkdown Report WF3-CS-12-00003 Rev 2 (Entergy, 2014). The goal of the walkdowns was to verify current plant configuration with the existing licensing basis, to verify the current maintenance plans, and to identify any vulnerabilities. The walkdown also verified that any vulnerabilities identified in the

IPEEE (Entergy, 2012) were adequately addressed. The results of the walkdown, including any identified corrective actions, confirm that WSES-3 can adequately respond to a seismic event.

6.0 Conclusions

In accordance with the 50.54(f) request for information (U.S. NRC, 2012), a seismic hazard and screening evaluation was performed for WSES-3. A GMRS was developed solely for the purpose of screening for additional evaluations in accordance with the SPID (EPRI, 2013a). Based on the results of the screening evaluation, WSES-3 screens-out for a seismic risk evaluation, a High Frequency Confirmation, and a Spent Fuel Pool evaluation.

7.0 References

- 10 CFR Part 50. Title 10, Code of Federal Regulations, Part 50, "Domestic Licensing of Production and Utilization Facilities," U.S. Nuclear Regulatory Commission, Washington DC.
- 10 CFR Part 50.72. Title 10, Code of Federal Regulations, Part 50.72, "Immediate Notification Requirements for Operating Nuclear Power Reactors," U.S. Nuclear Regulatory Commission, Washington DC.
- 10 CFR Part 50.73. Title 10, Code of Federal Regulations, Part 50.73, "Licensee Event Report System," U.S. Nuclear Regulatory Commission, Washington DC.
- 10 CFR Part 100. Title 10, Code of Federal Regulations, Part 100, "Reactor Site Criteria," U.S. Nuclear Regulatory Commission, Washington, DC.
- CEUS-SSC (2012). "Central and Eastern United States Seismic Source Characterization for Nuclear Facilities," U.S. Nuclear Regulatory Commission Report, NUREG-2115; EPRI Report 1021097, 6 Volumes; DOE Report DOE/NE-0140.
- Entergy (2012), "Waterford 3 Individual Plant Examination of External Events (IPEEE) Reduced Scope Seismic Margin Assessment (SMA). Report No. WF3-CS-12-00001, 02-07-2012/Revision, 0.
- Entergy (2013). "Waterford Steam Electric Station Final Safety Analysis Report Unit 3," Revision 307, Docket No. 50-382, 2013.
- Entergy (2014), "Waterford Steam Electric Station Unit 3 Seismic Walkdown Report for Resolution of Fukushima Near-Term Task Force Recommendation 2.3: Seismic." Engineering Report WF3-CS-12-00003, Rev. 2, 2013.
- EPRI (2012). "Seismic Walkdown Guidance for Resolution of Fukushima Near-Term Task Force Recommendation 2.3: Seismic," EPRI 1025286, June 2012.
- EPRI (2013a). "Seismic Evaluation Guidance Screening, Prioritization and Implementation Details (SPID) for the Resolution of Fukushima Near-Term Task Force Recommendation 2.1: Seismic," EPRI 1025287, February 2013.
- EPRI (2013b). "Seismic Evaluation Guidance: Augmented Approach for the Resolution of Fukushima Near-Term Task Force Recommendation 2.1 – Seismic," EPRI 3002000704, Final Report, May 2013.
- EPRI (2013c). "EPRI (2004, 2006) Ground-Motion Model (GMM) Review Project," EPRI 3002000717, 2 volumes, June 2013.

- EPRI (2014). "Waterford Seismic Hazard and Screening Report," Electric Power Research Institute, Palo Alto, CA, February 14, 2014.
- NEI (2013). NEI Letter to NRC, "Proposed Path Forward for NTF Recommendation 2.1: Seismic Reevaluations," April 9, 2013.
- NEI (2014). NEI Letter to NRC, "Seismic Risk Evaluations for Plants in the Central and Eastern United States," March 12, 2014.
- Toro (1997). Appendix of: Silva, W.J., Abrahamson, N., Toro, G., and Costantino, C. (1997). "Description and Validation of the Stochastic Ground Motion Model", Report Submitted to Brookhaven National Laboratory, Associated Universities, Inc., Upton, New York 11973, Contract No. 770573.
- U.S. NRC (2007). "A Performance-Based Approach to Define the Site-Specific Earthquake Ground Motion," U.S. Nuclear Regulatory Commission Reg. Guide 1.208.
- U.S. NRC (2010). "Implications of Updated Probabilistic Seismic Hazard Estimates in Central and Eastern United States on Existing Plants," GI-199, September 2, 2010.
- U.S. NRC (2012). NRC (E Leeds and M Johnson) Letter to All Power Reactor Licensees et al., "Request for Information Pursuant to Title 10 of the Code of Federal Regulations 50.54(f) Regarding Recommendations 2.1, 2.3 and 9.3 of the Near-Term Task Force Review of Insights from the Fukushima Dai-ichi Accident," March 12, 2012.
- U.S. NRC (2013). NRC Letter from E. Leeds to J. Pollock, "Electric Power Research Institute Final Draft Report XXXXXX, Seismic Evaluation Guidance: Augmented Approach for the Resolution of Fukushima Near-Term Task Force Recommendation 2.1: Seismic, as an Acceptable Alternative to the March 12, 2012, Information Request for Seismic Reevaluations," May 7, 2013.
- U.S. NRC (2014). NRC Letter, Eric J. Leeds to All Power Reactor Licensees, "Supplemental Information Related to Request for Information Pursuant to Title 10 of the Code of Federal Regulations 50.54(f) Regarding Seismic Hazard Reevaluations for Recommendation 2.1 of the Near-Term Task Force Review of Insights from the Fukushima Dai-Ichi Accident," dated February 20, 2014.

Appendix A

Tabulated Data

Table A-1a. Mean and Fractile Seismic Hazard Curves for PGA at WSES-3.
(EPRI, 2014)

| AMPS(g) | MEAN | 0.05 | 0.16 | 0.50 | 0.84 | 0.95 |
|---------|----------|----------|----------|----------|----------|----------|
| 0.0005 | 2.72E-02 | 1.42E-02 | 1.90E-02 | 2.68E-02 | 3.52E-02 | 4.19E-02 |
| 0.001 | 2.00E-02 | 9.24E-03 | 1.29E-02 | 1.92E-02 | 2.72E-02 | 3.33E-02 |
| 0.005 | 7.06E-03 | 2.19E-03 | 3.63E-03 | 6.45E-03 | 1.04E-02 | 1.38E-02 |
| 0.01 | 3.67E-03 | 9.51E-04 | 1.60E-03 | 3.14E-03 | 5.58E-03 | 8.23E-03 |
| 0.015 | 2.22E-03 | 5.50E-04 | 8.98E-04 | 1.77E-03 | 3.33E-03 | 5.58E-03 |
| 0.03 | 7.04E-04 | 1.60E-04 | 2.53E-04 | 4.98E-04 | 1.01E-03 | 2.04E-03 |
| 0.05 | 2.47E-04 | 4.56E-05 | 7.89E-05 | 1.67E-04 | 3.63E-04 | 7.45E-04 |
| 0.075 | 1.07E-04 | 1.55E-05 | 3.01E-05 | 7.03E-05 | 1.67E-04 | 3.28E-04 |
| 0.1 | 5.95E-05 | 7.34E-06 | 1.55E-05 | 3.90E-05 | 9.51E-05 | 1.84E-04 |
| 0.15 | 2.57E-05 | 2.72E-06 | 6.17E-06 | 1.67E-05 | 4.19E-05 | 8.00E-05 |
| 0.3 | 5.28E-06 | 4.01E-07 | 1.07E-06 | 3.37E-06 | 8.85E-06 | 1.64E-05 |
| 0.5 | 1.36E-06 | 7.77E-08 | 2.35E-07 | 8.35E-07 | 2.32E-06 | 4.37E-06 |
| 0.75 | 4.15E-07 | 1.72E-08 | 5.75E-08 | 2.39E-07 | 7.03E-07 | 1.44E-06 |
| 1. | 1.71E-07 | 4.98E-09 | 1.84E-08 | 8.98E-08 | 2.84E-07 | 6.36E-07 |
| 1.5 | 4.59E-08 | 7.66E-10 | 3.01E-09 | 1.98E-08 | 7.23E-08 | 1.98E-07 |
| 3. | 3.76E-09 | 1.49E-10 | 2.04E-10 | 1.02E-09 | 5.27E-09 | 1.98E-08 |
| 5. | 4.37E-10 | 1.11E-10 | 1.32E-10 | 2.01E-10 | 6.64E-10 | 2.64E-09 |
| 7.5 | 6.41E-11 | 1.11E-10 | 1.21E-10 | 1.72E-10 | 2.13E-10 | 5.12E-10 |
| 10. | 1.48E-11 | 1.11E-10 | 1.20E-10 | 1.72E-10 | 1.72E-10 | 2.29E-10 |

Table A-1b. Mean and Fractile Seismic Hazard Curves for 25 Hz at WSES-3.
(EPRI, 2014)

| AMPS(g) | MEAN | 0.05 | 0.16 | 0.50 | 0.84 | 0.95 |
|---------|----------|----------|----------|----------|----------|----------|
| 0.0005 | 2.84E-02 | 1.62E-02 | 2.10E-02 | 2.76E-02 | 3.63E-02 | 4.25E-02 |
| 0.001 | 2.14E-02 | 1.08E-02 | 1.44E-02 | 2.04E-02 | 2.88E-02 | 3.42E-02 |
| 0.005 | 8.63E-03 | 3.05E-03 | 4.63E-03 | 7.89E-03 | 1.25E-02 | 1.64E-02 |
| 0.01 | 5.00E-03 | 1.49E-03 | 2.35E-03 | 4.37E-03 | 7.55E-03 | 1.05E-02 |
| 0.015 | 3.30E-03 | 9.11E-04 | 1.44E-03 | 2.76E-03 | 5.05E-03 | 7.55E-03 |
| 0.03 | 1.12E-03 | 2.80E-04 | 4.37E-04 | 8.47E-04 | 1.64E-03 | 2.92E-03 |
| 0.05 | 3.42E-04 | 7.66E-05 | 1.25E-04 | 2.53E-04 | 5.12E-04 | 9.24E-04 |
| 0.075 | 1.28E-04 | 2.49E-05 | 4.50E-05 | 9.65E-05 | 2.01E-04 | 3.37E-04 |
| 0.1 | 7.01E-05 | 1.20E-05 | 2.32E-05 | 5.27E-05 | 1.11E-04 | 1.84E-04 |
| 0.15 | 3.38E-05 | 5.05E-06 | 1.11E-05 | 2.64E-05 | 5.50E-05 | 8.85E-05 |
| 0.3 | 1.09E-05 | 1.42E-06 | 3.42E-06 | 8.72E-06 | 1.79E-05 | 2.80E-05 |
| 0.5 | 4.50E-06 | 5.27E-07 | 1.31E-06 | 3.63E-06 | 7.66E-06 | 1.16E-05 |
| 0.75 | 2.06E-06 | 2.07E-07 | 5.58E-07 | 1.62E-06 | 3.52E-06 | 5.35E-06 |
| 1. | 1.12E-06 | 9.79E-08 | 2.88E-07 | 8.47E-07 | 1.95E-06 | 2.96E-06 |
| 1.5 | 4.29E-07 | 3.14E-08 | 9.51E-08 | 3.09E-07 | 7.55E-07 | 1.23E-06 |
| 3. | 6.27E-08 | 2.88E-09 | 9.37E-09 | 3.84E-08 | 1.10E-07 | 2.16E-07 |
| 5. | 1.17E-08 | 4.43E-10 | 1.25E-09 | 5.83E-09 | 2.01E-08 | 4.63E-08 |
| 7.5 | 2.61E-09 | 1.74E-10 | 2.96E-10 | 1.15E-09 | 4.43E-09 | 1.15E-08 |
| 10. | 8.20E-10 | 1.31E-10 | 1.77E-10 | 3.90E-10 | 1.42E-09 | 3.79E-09 |

Table A-1c. Mean and Fractile Seismic Hazard Curves for 10 Hz at WSES-3.
(EPRI, 2014)

| AMPS(g) | MEAN | 0.05 | 0.16 | 0.50 | 0.84 | 0.95 |
|---------|----------|----------|----------|----------|----------|----------|
| 0.0005 | 3.12E-02 | 1.95E-02 | 2.39E-02 | 3.01E-02 | 3.90E-02 | 4.56E-02 |
| 0.001 | 2.40E-02 | 1.34E-02 | 1.72E-02 | 2.32E-02 | 3.14E-02 | 3.73E-02 |
| 0.005 | 9.77E-03 | 4.01E-03 | 5.66E-03 | 9.11E-03 | 1.38E-02 | 1.77E-02 |
| 0.01 | 5.59E-03 | 1.95E-03 | 2.92E-03 | 5.05E-03 | 8.23E-03 | 1.08E-02 |
| 0.015 | 3.70E-03 | 1.18E-03 | 1.79E-03 | 3.28E-03 | 5.58E-03 | 7.66E-03 |
| 0.03 | 1.49E-03 | 4.37E-04 | 6.64E-04 | 1.21E-03 | 2.22E-03 | 3.47E-03 |
| 0.05 | 6.27E-04 | 1.74E-04 | 2.68E-04 | 4.98E-04 | 9.24E-04 | 1.53E-03 |
| 0.075 | 2.86E-04 | 7.13E-05 | 1.15E-04 | 2.22E-04 | 4.31E-04 | 7.03E-04 |
| 0.1 | 1.59E-04 | 3.47E-05 | 5.91E-05 | 1.23E-04 | 2.46E-04 | 4.01E-04 |
| 0.15 | 6.90E-05 | 1.15E-05 | 2.22E-05 | 5.20E-05 | 1.13E-04 | 1.82E-04 |
| 0.3 | 1.56E-05 | 1.72E-06 | 3.95E-06 | 1.10E-05 | 2.68E-05 | 4.50E-05 |
| 0.5 | 4.56E-06 | 4.19E-07 | 1.05E-06 | 3.14E-06 | 7.89E-06 | 1.34E-05 |
| 0.75 | 1.51E-06 | 1.21E-07 | 3.33E-07 | 1.04E-06 | 2.60E-06 | 4.50E-06 |
| 1. | 6.47E-07 | 4.63E-08 | 1.36E-07 | 4.50E-07 | 1.13E-06 | 1.95E-06 |
| 1.5 | 1.89E-07 | 1.01E-08 | 3.23E-08 | 1.23E-07 | 3.33E-07 | 6.09E-07 |
| 3. | 2.19E-08 | 4.25E-10 | 1.60E-09 | 1.01E-08 | 3.90E-08 | 8.60E-08 |
| 5. | 3.80E-09 | 1.69E-10 | 2.53E-10 | 1.40E-09 | 6.54E-09 | 1.69E-08 |
| 7.5 | 8.14E-10 | 1.21E-10 | 1.72E-10 | 3.33E-10 | 1.40E-09 | 3.95E-09 |
| 10. | 2.49E-10 | 1.11E-10 | 1.29E-10 | 1.90E-10 | 4.98E-10 | 1.36E-09 |

Table A-1d. Mean and Fractile Seismic Hazard Curves for 5.0 Hz at WSES-3.
(EPRI, 2014)

| AMPS(g) | MEAN | 0.05 | 0.16 | 0.50 | 0.84 | 0.95 |
|---------|----------|----------|----------|----------|----------|----------|
| 0.0005 | 3.57E-02 | 2.39E-02 | 2.80E-02 | 3.47E-02 | 4.37E-02 | 5.05E-02 |
| 0.001 | 2.93E-02 | 1.74E-02 | 2.16E-02 | 2.84E-02 | 3.73E-02 | 4.37E-02 |
| 0.005 | 1.25E-02 | 5.58E-03 | 7.66E-03 | 1.18E-02 | 1.74E-02 | 2.19E-02 |
| 0.01 | 7.30E-03 | 2.80E-03 | 4.07E-03 | 6.83E-03 | 1.05E-02 | 1.34E-02 |
| 0.015 | 4.91E-03 | 1.69E-03 | 2.53E-03 | 4.50E-03 | 7.23E-03 | 9.51E-03 |
| 0.03 | 2.04E-03 | 6.09E-04 | 9.51E-04 | 1.77E-03 | 3.09E-03 | 4.43E-03 |
| 0.05 | 8.93E-04 | 2.60E-04 | 3.95E-04 | 7.34E-04 | 1.31E-03 | 2.10E-03 |
| 0.075 | 4.22E-04 | 1.20E-04 | 1.84E-04 | 3.37E-04 | 6.09E-04 | 1.01E-03 |
| 0.1 | 2.39E-04 | 6.36E-05 | 1.02E-04 | 1.90E-04 | 3.52E-04 | 5.75E-04 |
| 0.15 | 1.04E-04 | 2.42E-05 | 4.13E-05 | 8.23E-05 | 1.60E-04 | 2.53E-04 |
| 0.3 | 2.30E-05 | 3.52E-06 | 7.13E-06 | 1.74E-05 | 3.79E-05 | 6.09E-05 |
| 0.5 | 6.66E-06 | 5.75E-07 | 1.38E-06 | 4.43E-06 | 1.18E-05 | 2.01E-05 |
| 0.75 | 2.17E-06 | 1.04E-07 | 2.88E-07 | 1.23E-06 | 3.95E-06 | 7.34E-06 |
| 1. | 8.80E-07 | 2.84E-08 | 9.24E-08 | 4.31E-07 | 1.62E-06 | 3.28E-06 |
| 1.5 | 2.10E-07 | 4.43E-09 | 1.64E-08 | 8.00E-08 | 3.84E-07 | 8.72E-07 |
| 3. | 1.31E-08 | 2.01E-10 | 4.56E-10 | 3.68E-09 | 2.22E-08 | 5.66E-08 |
| 5. | 1.71E-09 | 1.21E-10 | 1.72E-10 | 4.07E-10 | 2.49E-09 | 8.12E-09 |
| 7.5 | 3.56E-10 | 1.11E-10 | 1.21E-10 | 1.72E-10 | 5.27E-10 | 1.82E-09 |
| 10. | 1.13E-10 | 1.11E-10 | 1.21E-10 | 1.72E-10 | 2.49E-10 | 6.73E-10 |

Table A-1e. Mean and Fractile Seismic Hazard Curves for 2.5 Hz at WSES-3.
(EPRI, 2014)

| AMPS(g) | MEAN | 0.05 | 0.16 | 0.50 | 0.84 | 0.95 |
|---------|----------|----------|----------|----------|----------|----------|
| 0.0005 | 3.62E-02 | 2.46E-02 | 2.84E-02 | 3.52E-02 | 4.43E-02 | 5.12E-02 |
| 0.001 | 2.99E-02 | 1.79E-02 | 2.19E-02 | 2.92E-02 | 3.79E-02 | 4.50E-02 |
| 0.005 | 1.23E-02 | 5.66E-03 | 7.66E-03 | 1.16E-02 | 1.72E-02 | 2.13E-02 |
| 0.01 | 6.86E-03 | 2.68E-03 | 3.90E-03 | 6.45E-03 | 9.79E-03 | 1.25E-02 |
| 0.015 | 4.54E-03 | 1.55E-03 | 2.35E-03 | 4.19E-03 | 6.73E-03 | 8.72E-03 |
| 0.03 | 1.84E-03 | 4.90E-04 | 7.77E-04 | 1.53E-03 | 2.88E-03 | 4.19E-03 |
| 0.05 | 7.47E-04 | 1.79E-04 | 2.84E-04 | 5.75E-04 | 1.16E-03 | 1.92E-03 |
| 0.075 | 3.18E-04 | 7.23E-05 | 1.16E-04 | 2.39E-04 | 4.83E-04 | 8.60E-04 |
| 0.1 | 1.64E-04 | 3.63E-05 | 6.00E-05 | 1.23E-04 | 2.49E-04 | 4.43E-04 |
| 0.15 | 6.28E-05 | 1.31E-05 | 2.25E-05 | 4.70E-05 | 9.93E-05 | 1.67E-04 |
| 0.3 | 1.24E-05 | 1.90E-06 | 3.73E-06 | 9.11E-06 | 2.07E-05 | 3.37E-05 |
| 0.5 | 3.61E-06 | 3.73E-07 | 8.60E-07 | 2.46E-06 | 6.17E-06 | 1.07E-05 |
| 0.75 | 1.24E-06 | 7.77E-08 | 2.04E-07 | 7.23E-07 | 2.16E-06 | 4.13E-06 |
| 1. | 5.42E-07 | 2.01E-08 | 5.66E-08 | 2.68E-07 | 9.65E-07 | 2.01E-06 |
| 1.5 | 1.56E-07 | 1.87E-09 | 6.09E-09 | 5.50E-08 | 2.80E-07 | 6.45E-07 |
| 3. | 1.46E-08 | 1.31E-10 | 1.87E-10 | 2.22E-09 | 2.25E-08 | 7.03E-08 |
| 5. | 2.15E-09 | 1.11E-10 | 1.44E-10 | 2.49E-10 | 2.57E-09 | 1.04E-08 |
| 7.5 | 4.35E-10 | 1.11E-10 | 1.21E-10 | 1.72E-10 | 4.77E-10 | 2.01E-09 |
| 10. | 1.34E-10 | 1.11E-10 | 1.21E-10 | 1.72E-10 | 2.13E-10 | 6.45E-10 |

Table A-1f. Mean and Fractile Seismic Hazard Curves for 1.0 Hz at WSES-3.
(EPRI, 2014)

| AMPS(g) | MEAN | 0.05 | 0.16 | 0.50 | 0.84 | 0.95 |
|---------|----------|----------|----------|----------|----------|----------|
| 0.0005 | 3.23E-02 | 1.92E-02 | 2.39E-02 | 3.19E-02 | 4.07E-02 | 4.77E-02 |
| 0.001 | 2.52E-02 | 1.32E-02 | 1.74E-02 | 2.46E-02 | 3.28E-02 | 3.95E-02 |
| 0.005 | 9.59E-03 | 3.90E-03 | 5.75E-03 | 9.11E-03 | 1.32E-02 | 1.67E-02 |
| 0.01 | 5.49E-03 | 1.77E-03 | 2.88E-03 | 5.12E-03 | 8.12E-03 | 1.04E-02 |
| 0.015 | 3.79E-03 | 9.65E-04 | 1.69E-03 | 3.47E-03 | 5.83E-03 | 7.77E-03 |
| 0.03 | 1.75E-03 | 2.68E-04 | 5.20E-04 | 1.36E-03 | 3.05E-03 | 4.56E-03 |
| 0.05 | 7.93E-04 | 8.72E-05 | 1.77E-04 | 5.12E-04 | 1.44E-03 | 2.39E-03 |
| 0.075 | 3.50E-04 | 3.19E-05 | 6.54E-05 | 1.92E-04 | 6.17E-04 | 1.16E-03 |
| 0.1 | 1.75E-04 | 1.46E-05 | 3.05E-05 | 8.98E-05 | 2.92E-04 | 6.09E-04 |
| 0.15 | 5.69E-05 | 4.63E-06 | 9.51E-06 | 2.84E-05 | 8.85E-05 | 2.07E-04 |
| 0.3 | 6.73E-06 | 5.27E-07 | 1.15E-06 | 3.52E-06 | 1.08E-05 | 2.42E-05 |
| 0.5 | 1.49E-06 | 9.24E-08 | 2.25E-07 | 7.45E-07 | 2.53E-06 | 5.42E-06 |
| 0.75 | 5.02E-07 | 2.07E-08 | 5.66E-08 | 2.25E-07 | 8.35E-07 | 1.92E-06 |
| 1. | 2.38E-07 | 6.64E-09 | 2.04E-08 | 9.37E-08 | 3.90E-07 | 9.65E-07 |
| 1.5 | 8.26E-08 | 1.27E-09 | 4.37E-09 | 2.53E-08 | 1.31E-07 | 3.57E-07 |
| 3. | 1.24E-08 | 1.72E-10 | 3.09E-10 | 2.01E-09 | 1.69E-08 | 5.91E-08 |
| 5. | 2.72E-09 | 1.21E-10 | 1.72E-10 | 3.33E-10 | 2.96E-09 | 1.32E-08 |
| 7.5 | 7.41E-10 | 1.11E-10 | 1.21E-10 | 1.72E-10 | 7.13E-10 | 3.42E-09 |
| 10. | 2.77E-10 | 1.11E-10 | 1.21E-10 | 1.72E-10 | 3.05E-10 | 1.31E-09 |

Table A-1g. Mean and Fractile Seismic Hazard Curves for 0.5 Hz at WSES-3.
(EPRI, 2014)

| AMPS(g) | MEAN | 0.05 | 0.16 | 0.50 | 0.84 | 0.95 |
|---------|----------|----------|----------|----------|----------|----------|
| 0.0005 | 2.02E-02 | 1.08E-02 | 1.40E-02 | 1.95E-02 | 2.64E-02 | 3.19E-02 |
| 0.001 | 1.39E-02 | 6.83E-03 | 9.24E-03 | 1.32E-02 | 1.84E-02 | 2.25E-02 |
| 0.005 | 4.95E-03 | 1.36E-03 | 2.39E-03 | 4.63E-03 | 7.45E-03 | 9.65E-03 |
| 0.01 | 2.86E-03 | 4.43E-04 | 9.51E-04 | 2.49E-03 | 4.77E-03 | 6.64E-03 |
| 0.015 | 1.95E-03 | 1.98E-04 | 4.70E-04 | 1.53E-03 | 3.47E-03 | 5.05E-03 |
| 0.03 | 8.22E-04 | 4.01E-05 | 1.05E-04 | 4.63E-04 | 1.60E-03 | 2.76E-03 |
| 0.05 | 3.42E-04 | 1.04E-05 | 2.84E-05 | 1.40E-04 | 6.45E-04 | 1.34E-03 |
| 0.075 | 1.43E-04 | 3.33E-06 | 8.98E-06 | 4.63E-05 | 2.42E-04 | 6.09E-04 |
| 0.1 | 6.93E-05 | 1.42E-06 | 3.84E-06 | 1.98E-05 | 1.10E-04 | 3.01E-04 |
| 0.15 | 2.20E-05 | 4.25E-07 | 1.11E-06 | 5.58E-06 | 3.14E-05 | 9.51E-05 |
| 0.3 | 2.46E-06 | 4.70E-08 | 1.36E-07 | 6.26E-07 | 3.47E-06 | 1.05E-05 |
| 0.5 | 5.18E-07 | 8.35E-09 | 2.72E-08 | 1.32E-07 | 7.66E-07 | 2.32E-06 |
| 0.75 | 1.77E-07 | 1.95E-09 | 7.13E-09 | 3.95E-08 | 2.46E-07 | 8.47E-07 |
| 1. | 8.87E-08 | 7.23E-10 | 2.64E-09 | 1.67E-08 | 1.13E-07 | 4.43E-07 |
| 1.5 | 3.45E-08 | 2.35E-10 | 6.83E-10 | 4.63E-09 | 3.90E-08 | 1.79E-07 |
| 3. | 6.37E-09 | 1.23E-10 | 1.72E-10 | 5.05E-10 | 5.20E-09 | 3.33E-08 |
| 5. | 1.60E-09 | 1.11E-10 | 1.23E-10 | 1.90E-10 | 1.04E-09 | 7.77E-09 |
| 7.5 | 4.80E-10 | 1.11E-10 | 1.21E-10 | 1.72E-10 | 3.19E-10 | 2.16E-09 |
| 10. | 1.91E-10 | 1.11E-10 | 1.21E-10 | 1.72E-10 | 1.98E-10 | 8.85E-10 |

Table A-2. Amplification Functions for WSES-3. (EPRI, 2014)

| PGA | Median AF | Sigma In(AF) | 25 Hz | Median AF | Sigma In(AF) | 10 Hz | Median AF | Sigma In(AF) | 5 Hz | Median AF | Sigma In(AF) |
|----------|-----------|--------------|----------|-----------|--------------|----------|-----------|--------------|----------|-----------|--------------|
| 1.00E-02 | 2.02E+00 | 9.54E-02 | 1.30E-02 | 1.56E+00 | 9.47E-02 | 1.90E-02 | 1.47E+00 | 1.09E-01 | 2.09E-02 | 2.04E+00 | 1.65E-01 |
| 4.95E-02 | 1.27E+00 | 1.09E-01 | 1.02E-01 | 6.59E-01 | 1.10E-01 | 9.99E-02 | 1.07E+00 | 1.31E-01 | 8.24E-02 | 1.77E+00 | 1.82E-01 |
| 9.64E-02 | 1.04E+00 | 1.13E-01 | 2.13E-01 | 5.02E-01 | 1.14E-01 | 1.85E-01 | 9.27E-01 | 1.35E-01 | 1.44E-01 | 1.62E+00 | 1.85E-01 |
| 1.94E-01 | 8.41E-01 | 1.17E-01 | 4.43E-01 | 5.00E-01 | 1.19E-01 | 3.56E-01 | 7.60E-01 | 1.42E-01 | 2.65E-01 | 1.41E+00 | 1.85E-01 |
| 2.92E-01 | 7.37E-01 | 1.21E-01 | 6.76E-01 | 5.00E-01 | 1.23E-01 | 5.23E-01 | 6.57E-01 | 1.48E-01 | 3.84E-01 | 1.26E+00 | 1.86E-01 |
| 3.91E-01 | 6.68E-01 | 1.24E-01 | 9.09E-01 | 5.00E-01 | 1.26E-01 | 6.90E-01 | 5.83E-01 | 1.54E-01 | 5.02E-01 | 1.14E+00 | 1.90E-01 |
| 4.93E-01 | 6.15E-01 | 1.26E-01 | 1.15E+00 | 5.00E-01 | 1.28E-01 | 8.61E-01 | 5.25E-01 | 1.59E-01 | 6.22E-01 | 1.05E+00 | 1.96E-01 |
| 7.41E-01 | 5.28E-01 | 1.32E-01 | 1.73E+00 | 5.00E-01 | 1.34E-01 | 1.27E+00 | 5.00E-01 | 1.65E-01 | 9.13E-01 | 8.71E-01 | 2.07E-01 |
| 1.01E+00 | 5.00E-01 | 1.38E-01 | 2.36E+00 | 5.00E-01 | 1.40E-01 | 1.72E+00 | 5.00E-01 | 1.71E-01 | 1.22E+00 | 7.40E-01 | 2.15E-01 |
| 1.28E+00 | 5.00E-01 | 1.48E-01 | 3.01E+00 | 5.00E-01 | 1.49E-01 | 2.17E+00 | 5.00E-01 | 1.78E-01 | 1.54E+00 | 6.41E-01 | 2.27E-01 |
| 1.55E+00 | 5.00E-01 | 1.59E-01 | 3.63E+00 | 5.00E-01 | 1.60E-01 | 2.61E+00 | 5.00E-01 | 1.85E-01 | 1.85E+00 | 5.77E-01 | 2.35E-01 |
| 2.5 Hz | Median AF | Sigma In(AF) | 1 Hz | Median AF | Sigma In(AF) | 0.5 Hz | Median AF | Sigma In(AF) | | | |
| 2.18E-02 | 2.33E+00 | 1.58E-01 | 1.27E-02 | 3.42E+00 | 1.46E-01 | 8.25E-03 | 3.09E+00 | 1.66E-01 | | | |
| 7.05E-02 | 2.16E+00 | 1.70E-01 | 3.43E-02 | 3.27E+00 | 1.42E-01 | 1.96E-02 | 3.08E+00 | 1.57E-01 | | | |
| 1.18E-01 | 2.06E+00 | 1.73E-01 | 5.51E-02 | 3.18E+00 | 1.41E-01 | 3.02E-02 | 3.07E+00 | 1.53E-01 | | | |
| 2.12E-01 | 1.92E+00 | 1.74E-01 | 9.63E-02 | 3.04E+00 | 1.43E-01 | 5.11E-02 | 3.06E+00 | 1.49E-01 | | | |
| 3.04E-01 | 1.80E+00 | 1.76E-01 | 1.36E-01 | 2.93E+00 | 1.49E-01 | 7.10E-02 | 3.05E+00 | 1.48E-01 | | | |
| 3.94E-01 | 1.70E+00 | 1.80E-01 | 1.75E-01 | 2.84E+00 | 1.58E-01 | 9.06E-02 | 3.05E+00 | 1.51E-01 | | | |
| 4.86E-01 | 1.60E+00 | 1.84E-01 | 2.14E-01 | 2.76E+00 | 1.69E-01 | 1.10E-01 | 3.05E+00 | 1.54E-01 | | | |
| 7.09E-01 | 1.39E+00 | 1.90E-01 | 3.10E-01 | 2.63E+00 | 1.86E-01 | 1.58E-01 | 3.05E+00 | 1.70E-01 | | | |
| 9.47E-01 | 1.23E+00 | 2.02E-01 | 4.12E-01 | 2.55E+00 | 1.98E-01 | 2.09E-01 | 3.06E+00 | 1.89E-01 | | | |
| 1.19E+00 | 1.11E+00 | 2.12E-01 | 5.18E-01 | 2.49E+00 | 2.09E-01 | 2.62E-01 | 3.07E+00 | 2.05E-01 | | | |
| 1.43E+00 | 1.06E+00 | 2.19E-01 | 6.19E-01 | 2.44E+00 | 2.21E-01 | 3.12E-01 | 3.07E+00 | 2.16E-01 | | | |

Tables A-3a and A-3b are tabular versions of the typical amplification factors provided in Figures 2.3.6-1 and 2.3.6-2. Values are provided for two input motion levels at approximately 10^{-4} and 10^{-5} mean annual frequency of exceedance. These factors are unverified and are provided for information only. The figures should be considered the governing information.

Table A-3a. Median AFs and sigmas for Model 1, Profile 1, for 2 PGA levels.
For Information Only

| M1P1K1 | | Rock PGA=0.0495 | | M1P1K1 | | PGA=0.292 | |
|------------|---------|-----------------|--------------|------------|---------|-----------|--------------|
| Freq. (Hz) | Soil SA | med. AF | sigma ln(AF) | Freq. (Hz) | Soil SA | med. AF | sigma ln(AF) |
| 100.0 | 0.068 | 1.374 | 0.108 | 100.0 | 0.220 | 0.753 | 0.127 |
| 87.1 | 0.068 | 1.356 | 0.108 | 87.1 | 0.220 | 0.733 | 0.127 |
| 75.9 | 0.068 | 1.325 | 0.108 | 75.9 | 0.220 | 0.698 | 0.127 |
| 66.1 | 0.068 | 1.267 | 0.108 | 66.1 | 0.220 | 0.634 | 0.127 |
| 57.5 | 0.068 | 1.161 | 0.108 | 57.5 | 0.221 | 0.536 | 0.127 |
| 50.1 | 0.069 | 1.024 | 0.108 | 50.1 | 0.221 | 0.444 | 0.127 |
| 43.7 | 0.069 | 0.892 | 0.108 | 43.7 | 0.221 | 0.376 | 0.127 |
| 38.0 | 0.069 | 0.800 | 0.108 | 38.0 | 0.222 | 0.344 | 0.128 |
| 33.1 | 0.070 | 0.739 | 0.108 | 33.1 | 0.222 | 0.328 | 0.128 |
| 28.8 | 0.070 | 0.722 | 0.109 | 28.8 | 0.223 | 0.331 | 0.128 |
| 25.1 | 0.072 | 0.706 | 0.109 | 25.1 | 0.224 | 0.332 | 0.128 |
| 21.9 | 0.074 | 0.732 | 0.111 | 21.9 | 0.227 | 0.354 | 0.129 |
| 19.1 | 0.076 | 0.742 | 0.113 | 19.1 | 0.230 | 0.367 | 0.131 |
| 16.6 | 0.080 | 0.780 | 0.116 | 16.6 | 0.235 | 0.393 | 0.133 |
| 14.5 | 0.084 | 0.834 | 0.126 | 14.5 | 0.243 | 0.426 | 0.136 |
| 12.6 | 0.091 | 0.900 | 0.139 | 12.6 | 0.253 | 0.457 | 0.142 |
| 11.0 | 0.097 | 0.967 | 0.131 | 11.0 | 0.266 | 0.495 | 0.147 |
| 9.5 | 0.106 | 1.076 | 0.129 | 9.5 | 0.282 | 0.553 | 0.146 |
| 8.3 | 0.116 | 1.248 | 0.146 | 8.3 | 0.306 | 0.651 | 0.152 |
| 7.2 | 0.124 | 1.398 | 0.180 | 7.2 | 0.333 | 0.758 | 0.173 |
| 6.3 | 0.133 | 1.556 | 0.169 | 6.3 | 0.363 | 0.882 | 0.194 |
| 5.5 | 0.136 | 1.640 | 0.174 | 5.5 | 0.389 | 0.992 | 0.185 |
| 4.8 | 0.142 | 1.719 | 0.159 | 4.8 | 0.409 | 1.071 | 0.183 |
| 4.2 | 0.150 | 1.846 | 0.169 | 4.2 | 0.430 | 1.164 | 0.184 |
| 3.6 | 0.146 | 1.824 | 0.189 | 3.6 | 0.448 | 1.249 | 0.172 |
| 3.2 | 0.159 | 2.077 | 0.171 | 3.2 | 0.457 | 1.355 | 0.182 |
| 2.8 | 0.166 | 2.256 | 0.167 | 2.8 | 0.486 | 1.522 | 0.188 |
| 2.4 | 0.158 | 2.302 | 0.177 | 2.4 | 0.523 | 1.777 | 0.170 |
| 2.1 | 0.151 | 2.388 | 0.169 | 2.1 | 0.516 | 1.931 | 0.198 |
| 1.8 | 0.142 | 2.492 | 0.162 | 1.8 | 0.508 | 2.131 | 0.207 |
| 1.6 | 0.134 | 2.680 | 0.167 | 1.6 | 0.483 | 2.342 | 0.226 |
| 1.4 | 0.120 | 2.765 | 0.130 | 1.4 | 0.450 | 2.540 | 0.199 |
| 1.2 | 0.116 | 3.013 | 0.134 | 1.2 | 0.415 | 2.661 | 0.211 |
| 1.0 | 0.113 | 3.214 | 0.148 | 1.0 | 0.388 | 2.769 | 0.169 |
| 0.91 | 0.110 | 3.401 | 0.136 | 0.91 | 0.370 | 2.902 | 0.192 |
| 0.79 | 0.105 | 3.512 | 0.151 | 0.79 | 0.356 | 3.096 | 0.158 |
| 0.69 | 0.094 | 3.507 | 0.127 | 0.69 | 0.344 | 3.371 | 0.132 |
| 0.60 | 0.080 | 3.341 | 0.152 | 0.60 | 0.302 | 3.410 | 0.158 |
| 0.52 | 0.070 | 3.379 | 0.160 | 0.52 | 0.262 | 3.476 | 0.147 |
| 0.46 | 0.058 | 3.335 | 0.166 | 0.46 | 0.226 | 3.595 | 0.157 |
| 0.10 | 0.002 | 2.537 | 0.137 | 0.10 | 0.007 | 2.561 | 0.138 |

Table A-3b. Median AFs and sigmas for Model 2, Profile 1, for 2 PGA levels.
For Information Only

| M2P1K1 | | PGA=0.0495 | | M2P1K1 | | PGA=0.292 | |
|------------|---------|------------|--------------|------------|---------|-----------|--------------|
| Freq. (Hz) | Soil SA | med. AF | sigma ln(AF) | Freq. (Hz) | Soil SA | med. AF | sigma ln(AF) |
| 100.0 | 0.073 | 1.474 | 0.096 | 100.0 | 0.260 | 0.889 | 0.108 |
| 87.1 | 0.073 | 1.454 | 0.096 | 87.1 | 0.260 | 0.865 | 0.108 |
| 75.9 | 0.073 | 1.421 | 0.096 | 75.9 | 0.260 | 0.824 | 0.108 |
| 66.1 | 0.073 | 1.360 | 0.096 | 66.1 | 0.260 | 0.749 | 0.108 |
| 57.5 | 0.073 | 1.247 | 0.096 | 57.5 | 0.261 | 0.634 | 0.108 |
| 50.1 | 0.074 | 1.100 | 0.096 | 50.1 | 0.261 | 0.525 | 0.108 |
| 43.7 | 0.074 | 0.959 | 0.096 | 43.7 | 0.262 | 0.445 | 0.109 |
| 38.0 | 0.074 | 0.862 | 0.097 | 38.0 | 0.263 | 0.408 | 0.109 |
| 33.1 | 0.075 | 0.798 | 0.097 | 33.1 | 0.264 | 0.390 | 0.110 |
| 28.8 | 0.076 | 0.783 | 0.098 | 28.8 | 0.267 | 0.396 | 0.111 |
| 25.1 | 0.078 | 0.770 | 0.099 | 25.1 | 0.271 | 0.401 | 0.113 |
| 21.9 | 0.081 | 0.803 | 0.101 | 21.9 | 0.277 | 0.433 | 0.116 |
| 19.1 | 0.084 | 0.818 | 0.106 | 19.1 | 0.286 | 0.455 | 0.121 |
| 16.6 | 0.089 | 0.867 | 0.111 | 16.6 | 0.297 | 0.495 | 0.128 |
| 14.5 | 0.094 | 0.935 | 0.126 | 14.5 | 0.312 | 0.547 | 0.136 |
| 12.6 | 0.102 | 1.017 | 0.132 | 12.6 | 0.332 | 0.601 | 0.149 |
| 11.0 | 0.110 | 1.093 | 0.128 | 11.0 | 0.356 | 0.663 | 0.151 |
| 9.5 | 0.120 | 1.223 | 0.140 | 9.5 | 0.387 | 0.757 | 0.154 |
| 8.3 | 0.131 | 1.412 | 0.165 | 8.3 | 0.423 | 0.900 | 0.175 |
| 7.2 | 0.140 | 1.572 | 0.185 | 7.2 | 0.453 | 1.033 | 0.201 |
| 6.3 | 0.147 | 1.721 | 0.158 | 6.3 | 0.486 | 1.182 | 0.201 |
| 5.5 | 0.150 | 1.808 | 0.167 | 5.5 | 0.506 | 1.292 | 0.173 |
| 4.8 | 0.156 | 1.898 | 0.154 | 4.8 | 0.522 | 1.365 | 0.168 |
| 4.2 | 0.164 | 2.017 | 0.169 | 4.2 | 0.553 | 1.497 | 0.167 |
| 3.6 | 0.161 | 2.012 | 0.177 | 3.6 | 0.566 | 1.578 | 0.168 |
| 3.2 | 0.178 | 2.334 | 0.162 | 3.2 | 0.586 | 1.738 | 0.172 |
| 2.8 | 0.175 | 2.377 | 0.156 | 2.8 | 0.626 | 1.960 | 0.171 |
| 2.4 | 0.164 | 2.392 | 0.138 | 2.4 | 0.622 | 2.113 | 0.156 |
| 2.1 | 0.157 | 2.485 | 0.129 | 2.1 | 0.583 | 2.181 | 0.162 |
| 1.8 | 0.144 | 2.535 | 0.153 | 1.8 | 0.551 | 2.309 | 0.157 |
| 1.6 | 0.138 | 2.758 | 0.127 | 1.6 | 0.524 | 2.537 | 0.153 |
| 1.4 | 0.123 | 2.837 | 0.119 | 1.4 | 0.467 | 2.633 | 0.133 |
| 1.2 | 0.120 | 3.107 | 0.119 | 1.2 | 0.432 | 2.772 | 0.128 |
| 1.0 | 0.117 | 3.312 | 0.161 | 1.0 | 0.412 | 2.939 | 0.139 |
| 0.91 | 0.114 | 3.503 | 0.120 | 0.91 | 0.392 | 3.076 | 0.123 |
| 0.79 | 0.107 | 3.575 | 0.163 | 0.79 | 0.382 | 3.324 | 0.141 |
| 0.69 | 0.094 | 3.483 | 0.139 | 0.69 | 0.345 | 3.378 | 0.128 |
| 0.60 | 0.079 | 3.334 | 0.159 | 0.60 | 0.299 | 3.369 | 0.149 |
| 0.52 | 0.069 | 3.363 | 0.161 | 0.52 | 0.259 | 3.439 | 0.160 |
| 0.46 | 0.058 | 3.297 | 0.174 | 0.46 | 0.215 | 3.434 | 0.177 |
| 0.10 | 0.002 | 2.533 | 0.136 | 0.10 | 0.007 | 2.539 | 0.136 |